[American Journal of Science, Vol. 304, May, 2004, P. 397–437]

American Journal of Science

MAY 2004

COPSE: A NEW MODEL OF BIOGEOCHEMICAL CYCLING OVER PHANEROZOIC TIME

NOAM M. BERGMAN*, TIMOTHY M. LENTON** and ANDREW J. WATSON*

ABSTRACT. **We present a new model of biogeochemical cycling over Phanerozoic time. This work couples a feedback-based model of atmospheric O_2 and ocean nutrients (Lenton and Watson, 2000a, 2000b) with a geochemical carbon cycle model (Berner, 1991, 1994), a simple sulfur cycle, and additional components. The resulting COPSE model (Carbon-Oxygen-Phosphorus-Sulfur-Evolution) represents the co-evolution of biotic and abiotic components of the Earth system, in that it couples interactive and evolving terrestrial and marine biota to geochemical and tectonic processes. The model is forced with geological and evolutionary forcings and time-dependent solar insolation. The baseline model succeeds in giving simultaneous predictions of atmospheric O_2, CO_2, global temperature, ocean composition, $\delta^{13}C$ and $\delta^{34}S$ that are in reasonable agreement with available data and suggested constraints.**

The behavior of the coupled model is qualitatively different to single cycle models. While atmospheric pCO_2 (CO_2 partial pressure) predictions are mostly determined by the model forcings and the response of silicate weathering rate to pCO_2 and temperature, multiple negative feedback processes and coupling of the C, O, P and S cycles are necessary for regulating pO_2 while allowing $\delta^{13}C$ changes of sufficient amplitude to match the record.

The results support a pO_2 dependency of oxidative weathering of reduced carbon and sulfur, which raises early Paleozoic pO_2 above the estimated requirement of Cambrian fauna and prevents unrealistically large $\delta^{34}S$ variation. They do not support a strong anoxia dependency of the C:P burial ratio of marine organic matter (Van Cappellen and Ingall, 1994, 1996) because this dependency raises early Paleozoic $\delta^{13}C$ and organic carbon burial rates too high. The dependency of terrestrial primary productivity on pO_2 also contributes to oxygen regulation. An intermediate strength oxygen fire feedback on terrestrial biomass, which gives a pO_2 upper limit of ~1.6PAL (present atmospheric level) or 30 volume percent, provides the best combined pO_2 and $\delta^{13}C$ predictions.

Sulfur cycle coupling contributes critically to lowering the Permo-Carboniferous pCO_2 and temperature minimum. The results support an inverse dependency of pyrite sulfur burial on pO_2 (for example, Berner and Canfield, 1989), which contributes to the shuttling of oxygen back and forth between carbonate carbon and gypsum sulfur.

A pO_2 dependency of photosynthetic carbon isotope fractionation (Berner and others, 2000; Beerling and others, 2002) is important for producing sufficient magnitude of $\delta^{13}C$ variation. However, our results do not support an oxygen dependency of sulfur isotope fractionation in pyrite formation (Berner and others, 2000) because it generates unrealistically small variations in $\delta^{34}S$.

In the Early Paleozoic, COPSE predicts pO_2=0.2–0.6PAL and pCO_2>10PAL, with high oceanic [PO_4^{3-}] and low [$SO_4^{=}$]. Land plant evolution caused a 'phase change' in the Earth system by increasing weathering rates and shifting some organic burial to

*School of Environmental Sciences, University of East Anglia, Norwich NR4 7TJ, United Kingdom; n.bergman@uea.ac.uk

**Centre for Ecology and Hydrology, Edinburgh Research Station, Bush Estate, Penicuik, Midlothian EH26 0QB, United Kingdom

land. This change resulted in a major drop in pCO_2 to 3 to 4PAL and a rise in pO_2 to ~1.5PAL in the Permo-Carboniferous, with temperatures below present, ocean variables nearer present concentrations, and PO_4:NO_3 regulated closer to Redfield ratio. A second O_2 peak of similar or slightly greater magnitude appears in the mid-Cretaceous, before a descent towards PAL. Mesozoic CO_2 is in the range 3 to 7PAL, descending toward PAL in the Cretaceous and Cenozoic.

INTRODUCTION

COPSE *Model Concept*

We present a new biogeochemical model to examine possible coupled histories of O_2, CO_2 and other Phanerozoic Earth system variables. Where possible we have followed earlier models in order to facilitate comparison with earlier work. Thus, at the base of the model are the 'Redfield Revisited' models of Lenton and Watson (2000a, 2000b henceforth LW1 and LW2, respectively), feedback-based descriptions of atmosphere and ocean O_2 and ocean nutrients nitrate and phosphate. Carbon was included by coupling the model with major elements of the geological and geochemical Phanerozoic carbon cycle 'Geocarb' model of Berner (1991, 1994 henceforth B1 and B2, respectively). The model was also extended to include a simple sulfur cycle, based largely on Kump and Garrels (1986). The C and S cycles are each modeled with one reduced and one oxidized rock reservoir, and a smaller surficial reservoir. The model's C, O, P and S cycles are coupled through terrestrial and marine productivity and through biological and abiological weathering and deposition of C and S, in both reduced and oxidized states. The interactive biota includes marine productivity, dependent on NO_3 and PO_4, following LW1, and an interactive and evolving terrestrial biota, dependent on O_2 and CO_2. COPSE (Carbon, Oxygen, Phosphorus, Sulfur and Evolution) is a 'co-evolutionary' model of the Earth for geologic timescales.

Besides pCO_2 and pO_2, the model also gives semi-quantitative predictions of oceanic phosphate, nitrate, sulfate and calcium, and mean global temperature. Significantly, $\delta^{13}C$ and $\delta^{34}S$ records are *predicted*, rather than used as forcings, (in contrast to Garrels and Lerman, 1981, 1984; Kump, 1993; Berner and others, 2000) allowing comparison with independent geological data. Tectonic / geological and biogeochemical / evolutionary forcings are included, and feedback loops within the system are studied.

Our aim is to develop a 'co-evolutionary' biogeochemical model of the Earth system including evolving biota and geological processes. While the carbon and oxygen cycles are studied thoroughly herein, we acknowledge that further development is necessary. Specifically, future work on the model could include a more comprehensive sulfur cycle, more detailed ocean chemistry, and a more detailed inclusion of paleogeography.

Background: Phanerozoic Modeling

In a steady state model of the atmosphere-ocean-sediment system, Garrels and Perry (1974) demonstrated that the amount of O_2 and CO_2 cycled through the atmosphere during the past 600Ma has been much greater than the current content of the atmosphere. Garrels and Lerman (1984) similarly concluded that the atmosphere-ocean system acts more as a medium of transfer than as a reservoir in itself. Both O_2 and CO_2 levels are thought to be controlled by geological and biogeochemical feedbacks on a geological timescale. While the Phanerozoic history of both gases has been studied extensively, they have usually been studied separately. It is, however, apparent that many of the processes important to CO_2 history are also relevant to O_2.

Garrels and Lerman (1981, 1984) presented a simple sulfur and carbon cycle model, including sulfur reservoirs gypsum (oxidized) and pyrite (reduced), carbon reservoirs carbonate (oxidized) and organic carbon (reduced), and C and S in the

atmosphere-ocean system, with the appropriate weathering and burial fluxes. They concluded that "the exogenic geochemical cycles of carbon and sulfur can be, to a reasonably good first approximation, treated as a closed system" (Garrels and Lerman, 1984). The strong C-S coupling results in transfers among the sedimentary reservoirs far greater than the permissible changes in atmospheric levels of O_2 and CO_2, given the continued global presence of life. This 'shuttling' back and forth of oxygen between oxidized carbon and sulfur (carbonate and gypsum) may serve to regulate atmospheric pO_2. Berner and Canfield (1989) similarly model Phanerozoic pO_2 levels through the C and S cycles, with burial of organic matter and pyrite sulfur as the oxygen sources, and weathering of organic carbon and pyrite sulfur as the oxygen sinks. The only direct feedback on pO_2 in their model is via pyrite burial, which decreases with increasing pO_2.

The inverse covariance between $\delta^{13}C$ and $\delta^{34}S$ on a geological timescale (Veizer and others, 1980) also supports a link between the C and S cycles. Kump (1993) proposed that the general inverse relationship was the result of pyrite sulfur burial directly correlated to marine organic carbon burial, but inversely correlated to terrestrial organic carbon burial. Kump demonstrates the implications for models forced by carbon and sulfur isotope records. The coupling of the C, O and S cycles implies that simultaneous predictions of atmospheric pCO_2 and pO_2 should include the sulfur cycle.

The Geocarb models (B1, B2) successfully present a simple carbon cycle model, which yields predictions in fair agreement with Phanerozoic pCO_2 proxies. However, they do not account for the effects of changing pO_2 levels on the productivity of terrestrial biota, which in turn affects weathering rates and organic carbon burial rates. Geochemical pO_2 models must include at least the organic part of the C cycle (for example, Berner and Canfield, 1989; Berner and others, 2000; Lasaga and Ohmoto, 2002), but do not give simultaneous predictions of CO_2 and O_2. The Redfield Revisited models (LW1 and LW2) are feedback-based models that couple oxygen to ocean nutrients, and include an interactive biota, but do not include a full carbon cycle. Simultaneous Phanerozoic predictions of pO_2 and pCO_2 have to account for the combined effect of the two gases on the evolving terrestrial biota.

Oxygen Regulation

The regulating feedbacks for CO_2, as described by Walker and others (1981), by Berner and others (1983) and in the Geocarb models (B1, B2) have been accepted in much of the literature, at least as a good working hypothesis. However, despite much research, the control and regulation of atmospheric oxygen levels over geological time is still the subject of much controversy, with various processes proposed for pO_2 regulation.

Berner and Canfield (1989) proposed 'rapid recycling' of younger organic carbon and pyrite sulfur to improve oxygen regulation; according to this hypothesis, most weathering and sedimentation occurs in a relatively small pool of material, with a relatively short residence time. This idea was also used in Berner and others (2000). However, this mechanism was not used in carbon cycle models such as Geocarb, although it could have a significant effect on pCO_2 predictions.

Van Cappellen and Ingall (1994, 1996) found that phosphorus is more easily released from sediment in anoxic (or dysoxic) bottom waters, and concluded there could be a strong dependency of marine C:P burial ratio of organic matter on bottom-water anoxia, which in turn is a function of atmospheric pO_2. This dependency generates a negative feedback on atmospheric oxygen, which we refer to as the 'VCI' feedback. They assume a twenty-fold increase in C:P burial ratio between oxic and anoxic bottom waters, which has been questioned: Colman and others (1997) claim that data for modern marine sediments do not support this assumption, whereas

Anderson and others (2001) note that C_{org}:$P_{reactive}$ burial ratio (ratio of organic carbon burial to total burial of reactive phosphorus, both organic and inorganic) better describes the geochemical P cycle than C_{org}:P_{org}, and that C_{org}:$P_{reactive}$ does not vary as much between oxic and anoxic conditions. Kump and Mackenzie (1996) point out the problems of assuming one process regulating atmospheric pO_2 overwhelming all others.

Forest and grassland fires, reducing terrestrial productivity and biomass at high pO_2 levels, are proposed to regulate pO_2 in some models either by transferring P from land to ocean (Kump, 1993), or by reducing P weathering rates (LW2).

A pO_2 dependency of oxidative weathering of organic (reduced) carbon has been used in some models. Kump and Garrels (1986) used a linear dependency. Lasaga and Ohmoto (2002) deduce a weaker square root dependency, but Holland (2003) disputes the evidence for any pO_2 dependency, and many models (for example, LW1, LW2) assume the process is rapid enough that all exposed reduced material is oxidized.

COPSE MODEL DESCRIPTION

COPSE is a biogeochemical Earth system box model for the Phanerozoic, including the C, O, P and S cycles, and partial cycles for N and Ca. It includes geological processes of tectonic uplift, rock weathering and volcanic and metamorphic degassing; terrestrial and marine biota; burial of organic matter of both terrestrial and marine origin; and marine inorganic burial.

Both geological and evolutionary model forcings are included. The pre-industrial state of the Earth system is assumed to be a steady state attractor for modeling purposes, ensuring that the model gravitates towards it. Although the model is not usually at steady state, for a given set of forcings and parameters (held constant), the model gravitates toward a single steady state. Model runs are started with present-day reservoir sizes (ensuring mass conservation) at 600MaBP and are run for 50Myr with constant forcings representing the earliest Cambrian (550MaBP), bringing the model to near steady state. The runs continue from 550MaBP to present with forcings updated every million years. This type of modeling exercise is suited to long-term (multi-million year) events, but cannot capture more rapid episodic events.

The model allows many different hypotheses to be tested and compared by including different proposed flux functions and changing parameters, many of which can be altered at run time. In this paper only the chosen baseline and a few variations will be described, further variants are detailed in Bergman (ms, 2003). This baseline is a 'best guess', based on a combination of evaluation of different hypothesized feedbacks and comparison of resulting predictions to existing proxies and constraints on different parameters over the Phanerozoic. A description of model reservoirs, forcings and flux functions follows. Schematic diagrams of the model appear in figure 1.

Model Reservoirs

The model includes surface reservoirs of atmosphere and ocean oxygen (**O**) and CO_2 (**A**), and oceanic phosphate (**P**), nitrate (**N**), sulfate (**S**) and calcium (**CAL**). Crustal reservoirs of carbon and sulfur are also included, as organic (reduced) carbon (**G**), carbonate (oxidized) carbon (**C**), pyrite (reduced) sulfur (**PYR**) and gypsum (oxidized) sulfur (**GYP**). *In our notation*, upper case lettering (for example **GYP**) indicates reservoir size in moles, whereas lower case lettering (for example **gyp**) indicates size normalized to present. Model reservoirs are updated with each timestep in accordance with the flux functions, as detailed in table 1.

Model Forcings

COPSE includes six external forcings summarized in table 2. These include two geological forcings, tectonic uplift (***U***) and metamorphic and volcanic degassing (***D***), based on geological and geochemical proxies; a time-dependent insolation forcing (***I***); one evolutionary and tectonic forcing, the apportioning of carbonate burial between deep and shallow seas (***B***); and two terrestrial biota forcings representing evolution of vascular land plants and their colonization of the continents (***E***), and the resulting biological enhancement of weathering (***W***). All of the forcings except ***I*** are normalized to the present day, that is, at present ***U***, ***D***, ***E***, ***W***, ***B*** = 1. The baseline Phanerozoic history used for these five forcings is shown in figure 2. The insolation forcing is not calculated explicitly, but is used in the time dependent calculation of global temperature *T*.

Tectonic forcings.— The geological forcings are based on those used to force the Geocarb models (B1, B2). In the model baseline, two such forcings were introduced: ***D*** is modeled after Geocarb's (B2) tectonic degassing rate f_G. This approach follows that of the BLAG model (Berner and others, 1983): most decarbonation takes place as a result of subduction of sediments, therefore faster seafloor spreading rates (and subduction rates) will tend to increase decarbonation and therefore outgassing of CO_2; in turn, outgassing below continental interiors tends to increase worldwide tectonic activity. The BLAG model assumes a linear correlation of degassing to seafloor spreading rates. We follow B2 in using data from Engebretson and others (1992) for the past 150 million years and from Gaffin (1987) for the earlier Phanerozoic.

U is calculated as Geocarb's (B2) uplift factor f_R, using strontium isotope data from the Lowess fit (McArthur and others, 2001 and the accompanying computer-readable database) for the past 509 million years, and from Burke and others (1982) for the earlier Cambrian. ***U*** is tied linearly to weathering rates, following the Geocarb (B2) and Redfield Revisited (LW2) models' approach.

Geocarb's (B1, B2) other forcings were omitted from the baseline model (but see evolutionary forcings below). This omission was done in the interest of simplicity. It was found that the included forcings were sufficient to maintain the major results of Geocarb's pCO_2 predictions (high early Phanerozoic pCO_2, significant drop to a Permo-Carboniferous minimum and a Cretaceous maximum).

Evolutionary forcings.—***B*** attempts to capture the rise in carbonate degassing due to mid-Mesozoic rise of calcareous plankton, which are largely deposited in deep water. This process is thought to have increased carbonate susceptible to subduction, and hence thermal decomposition (Volk, 1989). ***B*** is taken from Geocarb (B1), and is given by:

$$\boldsymbol{B} = 0.75 \quad \text{from 550 MaBP to 150 MaBP}$$

$$\boldsymbol{B} = 0.75 + 0.25(1 - e^{-0.03(150-t)}) \quad \text{from 150 MaBP to present,} \qquad (1)$$

where t is time in MaBP.

The other biological forcings attempt to capture key changes in the evolution and spread of land plants and the resulting changes in the Earth system throughout the Phanerozoic. The biological forcings ***E*** and ***W*** are an attempt to quantify this history, specifically for two major events: first, the great rise of vascular land plants and their colonization of the Earth from the Silurian through the Carboniferous, and second, the rise of angiosperms in the Cretaceous. ***W*** represents weathering rate dependency on soil biological activity due to land plants, relative to the pre-vascular land plant world (*not* relative to abiotic conditions), and is modeled after Geocarb's f_E (B1, B2). ***E*** attempts to capture evolutionary development and spread of vascular land plants, and is used in calculating land productivity. Numbers between 0 and 1 were assigned for

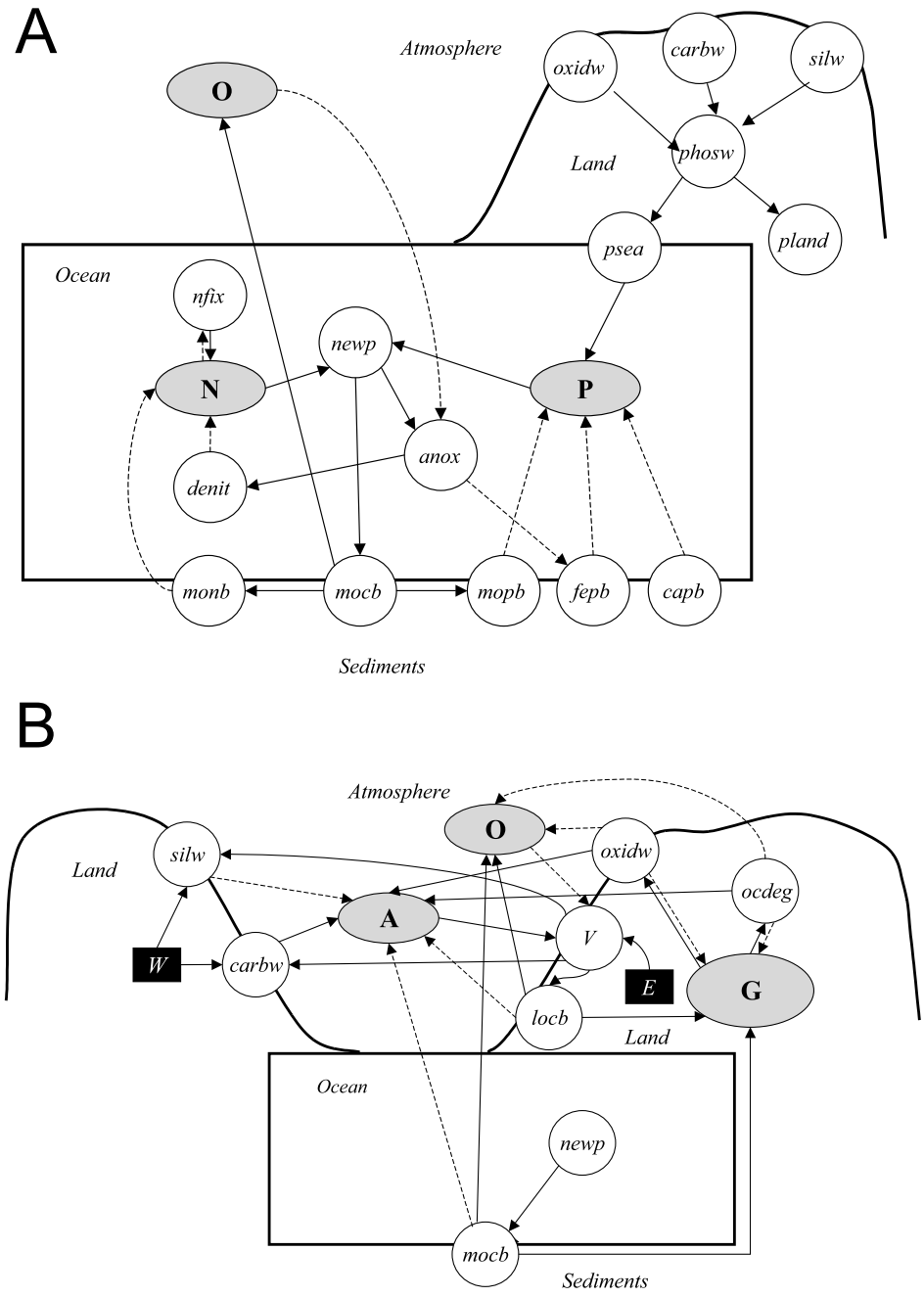

Fig. 1. COPSE model schemes. Circles indicate fluxes and other model parameters; shaded ovals – reservoirs; black rectangles – external forcings. Solid arrows indicate positive causality, dashed arrows, negative causality. A closed loop with an even number of dashed arrows (or none) shows a positive feedback loop; an odd number – a negative feedback loop. (A) P and N cycles. Reservoirs shown are ocean phosphate (**P**) and nitrate (**N**), and atmosphere and ocean O_2 (**O**). Fluxes and parameters are: oxidative weathering of organic carbon (*oxidw*), and weathering of carbonates (*carbw*), silicates (*silw*) and phosphorous (*phosw*); phosphorus flux to land (*pland*) and the oceans (*psea*); ocean fluxes denitrification (*denit*), nitrogen fixation (*nfix)* and new production (*newp*), and ocean parameter bottom water anoxia (*anox*); and marine burial fluxes of organic carbon (*mocb*), phosphate (*mopb*) and nitrate (*monb*) and inorganic phosphate burial as

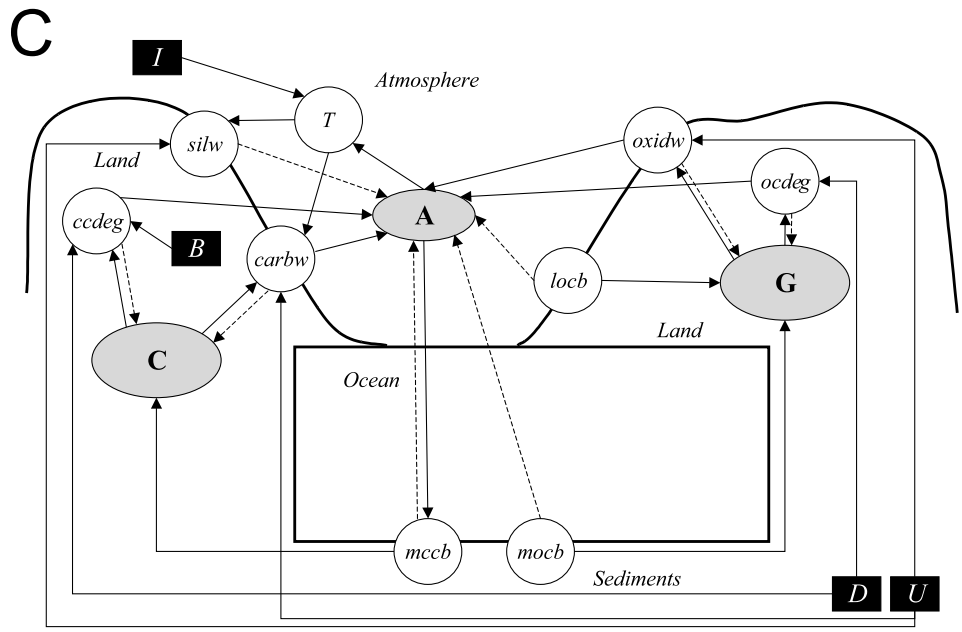

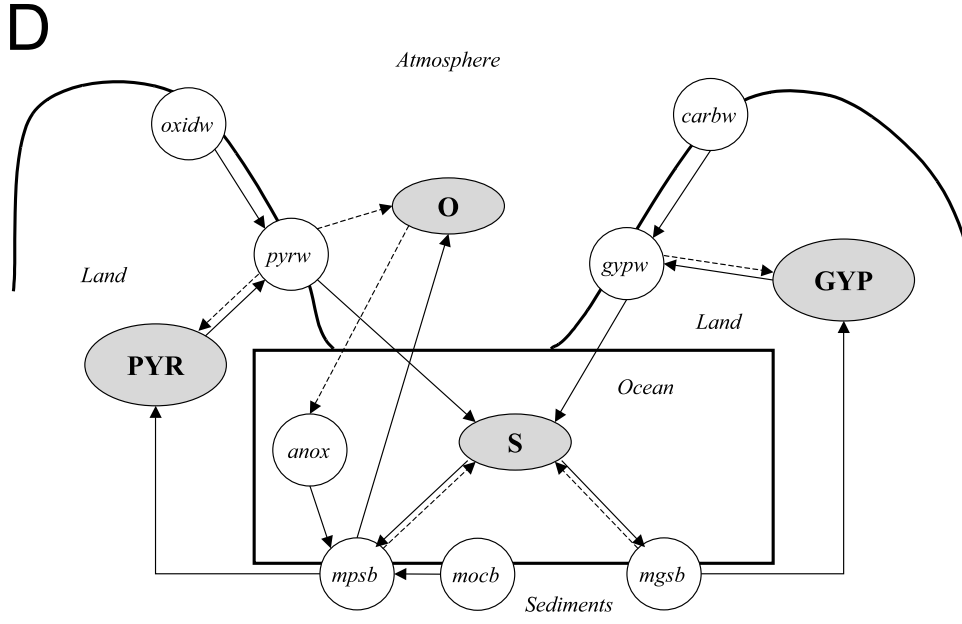

Fig. 1 (continued). calcium-bound (*capb*) and iron-sorbed (*fepb*). (B) Organic C and O cycles. Reservoirs include atmosphere and ocean CO_2 (**A**) and crustal organic (reduced) carbon (**G**). Fluxes and parameters include terrestrial vegetation (*V*) and organic carbon burial (*locb*), and degassing of organic carbon (*ocdeg*). Forcings shown are land plant evolution (***E***) and resulting enhancement of weathering (***W***). (C) Carbon cycle and inorganic forcings. Reservoirs include crustal carbonate (oxidized) carbon (**C**), fluxes include degassing of carbonate carbon (*ccdeg*), marine carbonate carbon burial (*mccb*), and the temperature parameter (*T*). Forcings shown are insolation (***I***), apportioning of carbonate burial between deep and shallow seas (***B***), tectonic uplift (***U***) and metamorphic and volcanic degassing (***D***). (D) The S cycle and calcium. Reservoirs include oceanic sulfate (**S**), crustal pyrite (reduced) sulfur (**PYR**), gypsum (oxidized) sulfur (**GYP**) and ocean calcium (**CAL**). Fluxes include weathering of gypsum (*gypw*) and pyrite (*pyrw*), and marine burial of sulfur as gypsum (*mgsb*) and pyrite (*mpsb*).

TABLE 1

The modeled reservoirs in COPSE. *The equations show the calculation of reservoir change with each timestep from the various flux functions*

Modeled Reservoir	**Equation (*d*reservoir/*dt*)**	Initial size
ocean phosphate (PO_4)	$\frac{d\mathbf{P}}{dt} = psea - mopb - fepb - capb$	$3.10 \cdot 10^{15}$ mol (2.2 μmol/kg)
bioavailable ocean nitrogen (NO_3)	$\frac{d\mathbf{N}}{dt} = nfix - denit - monb$	$4.35 \cdot 10^{16}$ mol (30.9 μmol/kg)
atmospheric and ocean O_2	$\frac{d\mathbf{O}}{dt} = locb + mocb - oxidw - ocdeg + 2 \cdot mpsb - 2 \cdot pyrw$	$3.70 \cdot 10^{19}$ mol
atmospheric and ocean CO_2	$\frac{d\mathbf{A}}{dt} = oxidw + ocdeg + carbw + ccdeg - locb - mocb - mccb$	$3.193 \cdot 10^{18}$ mol
crustal organic (reduced) carbon	$\frac{d\mathbf{G}}{dt} = locb + mocb - oxidw - ocdeg$	$1.25 \cdot 10^{21}$ mol
crustal carbonate (oxidized) carbon	$\frac{d\mathbf{C}}{dt} = mccb - carbw - ccdeg$	$5.00 \cdot 10^{21}$ mol
ocean sulfate	$\frac{d\mathbf{S}}{dt} = gypw + pyrw - mgsb - mpsb$	$4.0 \cdot 10^{19}$ mol (28.6 mmol/kg)
crustal pyrite (reduced) sulfur	$\frac{d\mathbf{PYR}}{dt} = mpsb - pyrw$	$1.8 \cdot 10^{20}$ mol
crustal gypsum (oxidized) sulfur	$\frac{d\mathbf{GYP}}{dt} = mgsb - gypw$	$2.0 \cdot 10^{20}$ mol
ocean calcium	$\frac{d\mathbf{CAL}}{dt} = silw + carbw + gypw - mccb - mgsb$	$1.397 \cdot 10^{19}$ mol (10 mmol/kg)

each stage of evolutionary development, with linear interpolation in between. This is a crude quantification, but it was found that the exact functions describing $\boldsymbol{E}$ and $\boldsymbol{W}$ throughout the two major events had little effect on model results. The land plant evolutionary history used follows Stanley (1999).

In the early Phanerozoic, before the evolution of land plants, $\boldsymbol{E} = 0$ and therefore their effect on weathering $\boldsymbol{W} = 0$. $\boldsymbol{E}$ is 0 throughout the Cambrian, and rises mostly during the Devonian and Carboniferous, up to 1 in the Late Carboniferous, when widespread forests covered the earth. $\boldsymbol{W}$ rises only to 0.75 in the late Carboniferous; only after weathering rates are increased by angiosperms in the Late Cretaceous (B1, and references therein) does $\boldsymbol{W}$ rise to 1.

TABLE 2

The six modeled forcings in COPSE. *The geological forcings,* ***D*** *and* ***U****, and the biological/evolutionary forcings,* ***E****,* ***W*** *and* ***B****, are normalized.*

Forcing	Modeled process	Phanerozoic range of values	Source
D	metamorphic and volcanic degassing	0.98 – 1.73	Geocarb method (B2); data from Gaffin (1987) & Engebretson and others (1992)
U	tectonic uplift	0.53 – 1.17	Geocarb method (B2); data from Burke and others (1982) & McArthur and others (2001)
E	land plant evolution and land colonization	0 (Cambrian) – 1 (Permian – Present)	Bergman (2003)
W	land plant enhancement of weathering	0 (Cambrian) – 1 (Late Cretaceous – Present)	adapted from Geocarb (B1)
B	apportioning of carbonate burial between deep and shallow seas	0.75 (Cambrian – Late Jurassic) – 1 (Present)	Geocarb (B1)
I	insolation (solar luminosity)	~4.4% increase over the Phanerozoic	Caldeira and Kasting (1992)

Atmospheric pCO_2 and Global Temperature

Atmospheric CO_2 is considered to be a constant fraction of the atmosphere and ocean CO_2 reservoir ***A***. This procedure makes normalized **a** the same as pCO_2 (in PAL). The temperature variable T represents mean global surface temperature, with present (pre-industrial) temperature taken to be $T_0 = 15\,^{\circ}C$. Only time-dependent solar insolation and atmospheric pCO_2 are used in temperature calculation, providing an inexact estimate. This method requires iteration in calculating T.

We use the energy balance model of Caldeira and Kasting (1992) to calculate T. This detailed model accounts for changing albedo levels with temperature, a greenhouse warming factor that is a function of both pCO_2 levels and ambient temperature, and solar luminosity that increases nonlinearly with time. Present day time ($t = 0$) and pCO_2 yield a converging value of $T = 14.24\,^{\circ}C$. Values were amended in COPSE to yield $T = 15.0\,^{\circ}C$ for present day values. The induced error to the model calculations is estimated at $< 0.15\,^{\circ}C$.

Land Biota

Comparatively few models of this type have an explicit land plant variable such as COPSE's V, which represents land plant coverage and biomass, and organic carbon thus produced. V is normalized, and relative changes in V are compared. No attempt is made to model different types of plants, beyond estimates for the biological forcings ***E*** and ***W***. We first consider the effects of land primary productivity, for which an auxiliary (normalized) parameter V_{npp} is defined; considerations of oxygen dependent fire frequency are then added afterwards. We have explored both a global (or 'macro-

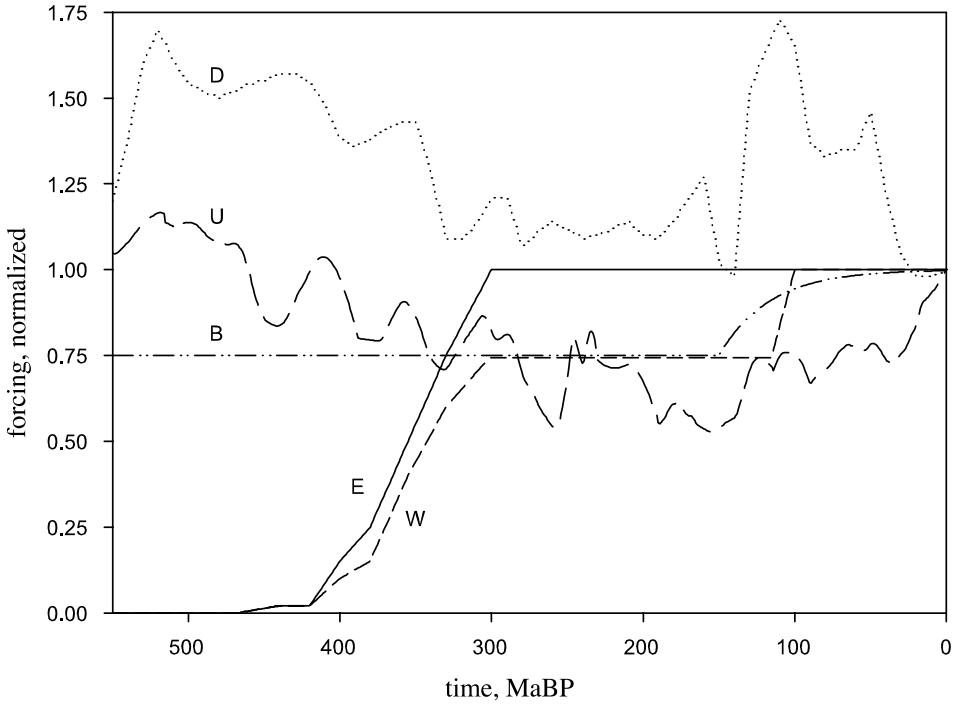

Fig. 2. Geological and biological external forcings: ***D***, metamorphic and volcanic degassing; ***U***, tectonic uplift; ***B***, carbon burial apportioning between shallow and deep ocean; ***E***, land plant evolution and land colonization; and ***W***, resulting biological enhancement of weathering. All five forcings are normalized, that is, at present they equal 1.

scopic') and a biochemical (or 'microscopic') approach to modeling net primary productivity. Modeling V_{npp} poses a challenge because studies of leaves or whole plants cannot always be extended to entire ecosystems, and extant plants are not necessarily a faithful indication of plant productivity under similar conditions in past geological periods.

A simple global approach was taken first (the '*OCT*' feedback). This approach was later compared to a biochemical approach, following Farquhar and others (1980) and Friend and others (1998) (the '*Friend*' feedback, detailed in appendix 2). The Friend feedback yields more complex functions, with a problematic extrapolation from cellular biology to global biota. The predictions it yielded were similar to or worse than those using the OCT feedback. Hence the OCT feedback was chosen for the COPSE baseline.

The OCT feedback.—Photosynthetic production on land was assumed to depend on $p\mathrm{CO}_2$, $p\mathrm{O}_2$ and global temperature. We based this function on the global productivity function of Caldeira and Kasting (1992), whose function is the product of a temperature term and a $p\mathrm{CO}_2$ term. The temperature factor assumes maximum productivity at 25°C, decreasing to zero at 0°C and 50°C (Volk, 1987; Caldeira and Kasting, 1992):

$$V_{npp}(T) = 1 - \left(\frac{T - 25}{25}\right)^2 \tag{2}$$

The $p\mathrm{CO}_2$ dependency is assumed to follow a Michaelis-Menten equation (Volk, 1987):

$$V_{npp}(\mathrm{CO_2}) = \frac{P_{atm} - P_{\min}}{P_{1/2} + (P_{atm} - P_{\min})} \tag{3}$$

where P_{atm} is atmospheric $p\mathrm{CO_2}$, P_{min} is the minimum atmospheric $p\mathrm{CO_2}$ under which plants can grow, taken to be 10 ppm (as for C4 plants in Caldeira and Kasting, 1992) and $P_{1/2}$ = 183.6 ppm, adopted so that the maximum productivity possible is twice pre-industrial levels ($V_{npp}(T) \cdot V_{npp}(CO_2) = 0.5$ at T_0 = 15 °C, $p\mathrm{CO_2}$ = 280 ppm).

We add to this equation an expression for oxygen, which inhibits land primary productivity, both through competition with $\mathrm{CO_2}$ for sites on the Rubisco enzyme, and through oxygen toxicity (Fridovich, 1998). This inhibition of $\mathrm{C_3}$ plant growth is sometimes known as the 'Warburg effect' (Fridovich, 1977), and we follow the quantification of the Redfield Revisited (LW2) model:

$$V_{npp}(\mathrm{O_2}) = 1.5 - 0.5 \cdot \mathbf{o} \tag{4}$$

LW2 use atmospheric oxygen mixing ratio, but in COPSE, (normalized) atmospheric $p\mathrm{O_2}$ content **o** is used, the logic being that the $\mathrm{O_2}$:$\mathrm{CO_2}$ ratio is significant in primary productivity rates, while $\mathrm{O_2}$:$\mathrm{N_2}$ ratio is not. In practice, it was found there was little difference between the two methods, except at high $p\mathrm{O_2}$ levels.

The three dependency terms are multiplied together, and the combined $\mathrm{O_2}$, $\mathrm{CO_2}$ and T dependency will be referred to as the 'OCT' feedback. The overall calculation of V_{npp} is therefore:

$$V_{npp} = 2\boldsymbol{E} \cdot V_{npp}(\mathrm{O_2}) \cdot V_{npp}(T) \cdot V_{npp}(\mathrm{CO_2}) \tag{5}$$

Note that the COPSE evolutionary forcing $\boldsymbol{E}$ has been added, as well as a factor of 2 for normalization.

Fire feedback.—The effect of fires on land biota is also included. The baseline fire feedback follows LW2:

$$\mathbf{O}' = \frac{\mathbf{o}}{\mathbf{o} + k_{16}} \tag{6}$$

$$ignit = max(586.2 \cdot \mathbf{O}' - 122.102, 0) \tag{7}$$

$$V = V_{npp} \cdot \frac{k_{fire}}{k_{fire} - 1 + ignit} \tag{8}$$

Equation (6) translates normalized **o** to atmospheric oxygen mixing ratio $\mathbf{O}'$, with k_{16} = 3.762, ensuring that $\mathbf{O}'$ = 0.21 for **o** = 1. In equation (7), *ignit* represents the ignition component, an indicator of fire probability that depends approximately linearly on $p\mathrm{O_2}$ (LW2), following the work of Watson (ms, 1978). Equation (8) is the proposed long-term effect of fires on land biomass. V represents land biomass after taking into account the effect of fires. LW2 has a strong fire feedback, with fire frequency constant k_{fire}= 20.

Some other models (for example, Kump, 1993) also include a fire effect on land biota as part of an important feedback regulating atmospheric $p\mathrm{O_2}$, but this idea has also met with much resistance. Robinson (1989) states that oxygen fuelled fires have shaped terrestrial evolution since the Carboniferous, and details various mechanisms through which plants can adapt to high oxygen and frequent fire conditions. However, survival in frequent fire conditions is not the question: it is whether the intense growth needed to bury the large amounts of organic carbon in the Carboniferous could have thrived in high oxygen conditions. Beerling and others (1998) offer some resolution in proposing that high $p\mathrm{O_2}$ levels would result in most land biota experiencing frequent

fires, with moist swamp regions establishing more mature vegetation. This proposal would suggest extreme differences between great coal swamps and other terrestrial ecosystems, perhaps not incompatible with proposed Late Carboniferous zonality and high polar-equator climate gradients (for example, Frakes, 1979). In this paper we take the view that while some adaptation to high pO_2 is possible, this would involve a trade-off, with fire resistance coming at the expense of productivity, or adaptation to frequent fires reducing total biomass. Thus, k_{fire} also represents possible adaptations of land biota that could reduce the effects of fire on net primary productivity. The baseline uses a much weaker fire feedback than used in LW2, with $k_{fire} = 100$. The effect of fires is also compared to having no fire feedback at all, that is:

$$V = V_{npp} \tag{9}$$

Weathering and Degassing Fluxes

Carbon degassing fluxes.—The degassing fluxes, carbonate degassing (*ccdeg*) and organic carbon degassing (*ocdeg*), express metamorphic and volcanic release of carbon to the atmosphere/ocean system. These fluxes were taken from B1:

$$ccdeg = k_{12} \cdot \boldsymbol{D} \cdot \boldsymbol{B} \cdot \mathbf{c} \tag{10}$$

$$ocdeg = k_{13} \cdot \boldsymbol{D} \cdot \mathbf{g} \tag{11}$$

where **c** and **g** are normalized reservoirs **C** and **G**. The constants k_{12} and k_{13} are obtained by multiplying Geocarb's k_{mc} and k_{mg}, respectively, by the present (t=0) size of the appropriate carbon reservoir ($\mathbf{C}_0$ and $\mathbf{G}_0$, respectively). *In our notation*, italics mark fluxes and parameters (for example, *ccdeg*) and prime a normalized flux (that is, $ccdeg' = ccdeg/ccdeg_0$).

Silicate and carbonate weathering.—Silicate and carbonate weathering fluxes (*silw*, *carbw*) account both for weathering rate dependency on tectonic activity, and for the biological amplification of weathering. The calculations follow the weathering functions of the Geocarb models (B1, B2), but with a co-evolutionary approach including an interactive biota, following the Redfield Revisited models (LW1, LW2).

The tectonic effect on weathering rates was expressed using uplift forcing $\boldsymbol{U}$ taken from Geocarb (B1, B2). The biological effects are divided into two: direct effect on weathering from increased number of land plants and their evolution and development of roots; and a change in weathering rate response to atmospheric pCO_2 due to the increased biological activity in soil (f_{CO_2}, g_{CO_2}). Both biological effects are dependent on land productivity, *V*, rather than on forcing parameters alone, in contrast to the Geocarb models. The resulting silicate weathering baseline function:

$$silw = k_{12} \cdot \boldsymbol{U} \cdot f_{CO_2[k_{15}+(1-k_{15})W \cdot V]} \tag{12}$$

and carbonate weathering baseline function:

$$carbw = k_{14} \cdot \boldsymbol{U} \cdot g_{CO_2[k_{15}+(1-k_{15})W \cdot V]} \tag{13}$$

where k_{14} is obtained by multiplying Geocarb's k_{wc} by $\mathbf{C}_0$, and k_{15}=0.15 expresses the pre-land plant weathering rate; that is, $1/k_{15}$ is the land plant amplification of weathering rates, taken to be ~7 (B1). The term in square brackets thus expresses an increase from k_{15} (with no plants) to 1 (at V=1) in direct biological weathering with the evolution of land plants. Later versions of the Geocarb model (B2) assume relief plays little role in carbonate dissolution (Holland, 1978), equivalent here to removing $\boldsymbol{U}$ from equation (13). In COPSE it was found that this assumption greatly reduced the oxygen constraints, leading to unrealistically high pO_2 in the Mesozoic and Cenozoic

(Bergman, ms, 2003). The baseline model therefore includes ***U*** in the carbonate weathering equation.

The weathering responses to temperature and $p\mathrm{CO}_2$ levels (f_{CO_2}, g_{CO_2}) are adapted from B2 and from Berner and others (1983): different temperature dependencies for silicate and carbonate weathering, but similar direct CO_2 response. The CO_2 dependency uses two different functions, one for the pre-vascular land plant dependency and one for dependency with plants present. We depart from B2 in the temperature calculation, which is separate and follows Caldeira and Kasting (1992). The calculation for silicate weathering is as follows:

$$f_T = e^{0.090(T-T_0)}[1 + 0.038(T - T_0)]^{0.65} \tag{14}$$

$$f_{pre\text{-}plant} = f_T\sqrt{\mathbf{a}} \tag{15}$$

$$f_{plant} = f_T\left(\frac{2\mathbf{a}}{1+\mathbf{a}}\right)^{0.4} \tag{16}$$

$$f_{CO2} = f_{pre\text{-}plant}(1 - VW) + f_{plant}VW \tag{17}$$

where $f_{pre\text{-}plant}$ is the pre-land plant dependency, f_{plant} is the dependency when land plants are present, and VW is here the minimum of $V \cdot \boldsymbol{W}$ or 1 (both V and $\boldsymbol{W}$ are normalized). Equation (17) departs from Geocarb: Berner uses equation (15) up to 350MaBP, equation (16) from 300MaBP onwards, and a linear interpolation from 350 to 300MaBP; COPSE does not use an explicitly time-dependent interpolation, rather, the biologically influenced response to $p\mathrm{CO}_2$ is re-calculated at every step, based on land productivity V and biological weathering enhancement $\boldsymbol{W}$. For carbonate weathering, a different temperature dependency function is used (B2):

$$g_T = 1 + 0.087(T - T_0) \tag{18}$$

but otherwise the calculation is the same for $\mathrm{g}_{\text{pre-plant}}$ and $\mathrm{g}_{\text{plant}}$, and therefore:

$$g_{CO_2} = g_{pre\text{-}plant}(1 - VW) + g_{plant}VW \tag{19}$$

Following Geocarb (B1, B2), oceanic carbonate is assumed to be at steady state, with marine carbonate burial (mccb) balancing carbonate input through silicate and carbonate weathering:

$$mccb = silw + carbw. \tag{20}$$

This relationship effectively assumes constant (super)saturation with respect to carbonate minerals; a more detailed ocean carbonate chemistry would be more realistic, but was not included in this version of the model.

Oxidative weathering of organic carbon.—The oxidative weathering flux (*oxidw*) follows the Geocarb formula of linear dependency on the organic carbon reservoir **G** and tectonic uplift forcing ***U***. The present rate of oxidative weathering is calculated assuming steady state. The baseline model also includes a weak (square root) dependency of oxidative weathering on $p\mathrm{O}_2$, taken from Lasaga and Ohmoto (2002). The baseline function is therefore:

$$oxidw = k_{17} \cdot \boldsymbol{U} \cdot \mathbf{g} \cdot \sqrt{\mathbf{o}} \tag{21}$$

where k_{17} is the oxidative weathering constant, determined by present steady state, **g** is normalized **G**, and **o** is normalized **O** (that is, $p\mathrm{O}_2$ in PAL).

An alternative function with no $p\mathrm{O}_2$ dependency of oxidative weathering is also explored, due to the uncertainty surrounding this feedback:

$$oxidw = k_{17} \cdot \boldsymbol{U} \cdot \mathbf{g} \tag{22}$$

Sulfur weathering.—It is assumed that weathering fluxes of gypsum and pyrite sulfur can be approximated by associating them with carbonate, silicate or oxidative weathering. The gypsum weathering flux *gypw* was made proportional to the carbonate weathering flux *carbw*, assuming gypsum is weathered similarly to carbonates. The function is therefore:

$$gypw = k_{22} \cdot \mathbf{gyp} \cdot carbw' = k_{22} \cdot \mathbf{gyp} \cdot \boldsymbol{U} \cdot \mathbf{g}_{CO_2}[k_{15} + (1 - k_{15})\boldsymbol{W} \cdot V] \tag{23}$$

where k_{22} is a constant representing present rates of weathering, **gyp** is the normalized oxidized sulfur reservoir (**GYP**), and *carbw'* normalized carbonate weathering.

The pyrite weathering flux *pyrw* is modeled after the oxidative weathering of organic carbon *oxidw* in the baseline. This approach builds a symmetry between the carbon cycle and the sulfur cycle: oxidized sulfur (**GYP**) is weathered with oxidized carbon (**C**), and reduced sulfur (**PYR**) with reduced carbon (**G**). Kump and Garrels (1986) have such a symmetry in their C-S-O model, with oxidative weathering of both carbon and sulfur linearly dependent on pO_2. Making *pyrw* and *oxidw* depend on the same parameters is also in line with the coupled carbon and sulfur model of Berner and Canfield (1989). Following *oxidw*, the function is:

$$pyrw = k_{21} \cdot \boldsymbol{U} \cdot \mathbf{pyr} \cdot \sqrt{\mathbf{o}} \tag{24}$$

where k_{21} is a constant representing present rates of weathering and **pyr** is the normalized reduced sulfur reservoir (**PYR**). In runs where the oxygen dependency of *oxidw* is removed, it is removed from *pyrw* as well for consistency.

Phosphorus weathering.—COPSE has three marine phosphorus burial fluxes: organic, calcium-bound and iron-sorbed, following LW1. These forms of phosphorus are assumed to contribute to phosphorus weathering in proportions similar to their burial fluxes, following the analysis of Van Cappellen and Ingall (1994, 1996). Organically buried phosphorus is assumed to be weathered with organic matter, and is associated with oxidative weathering of reduced carbon. Calcium-bound phosphorus is buried with carbonates, and is assumed to be weathered with them. Iron-sorbed phosphorus is assumed to be weathered with igneous and metamorphic silicates. The relative proportions of Org-P : Ca-P : Fe-P were taken to be = 5:5:2, respectively (Van Cappellen and Ingall, 1994, 1996). Thus COPSE closes the phosphorus cycle, with the three forms of burial matched with the three rock weathering fluxes. The baseline phosphorus weathering function is therefore:

$$phosw = k_{10}\left(\tfrac{2}{12}\, silw' + \tfrac{5}{12}\, carbw' + \tfrac{5}{12}\, oxidw'\right) \tag{25}$$

Note that this analysis ignores the phosphorus to land flux (*pland*), which is buried entirely as terrestrially derived organic matter. However, this flux is considerably smaller than the marine organic phosphorus burial (*mopb*), and the ratios in equation (25) remain reasonably accurate.

Phosphorus and Terrestrial Organic Burial

Phosphate to land and sea.—The input of reactive weathered phosphorus (*phosw*) is divided between two fluxes, with most going into the ocean (*psea*), but a small fraction L buried with land plant matter (*pland*), following Kump (1988) and LW2. L is assumed to vary linearly with the terrestrial vegetation, V:

$$L = k_{11} V \tag{26}$$

k_{11} is determined by steady state, and is larger than LW2's k_{12}, after which it is modeled, due to larger organic burial fluxes assumed in COPSE. The phosphorus fluxes are given by:

$$pland = L \cdot phosw = k_{11} \cdot V \cdot phosw \tag{27}$$

$$psea = (1 - L)phosw = (1 - k_{11}V)phosw \tag{28}$$

Land organic carbon burial.—The flux of terrestrially-derived organic carbon burial (*locb*) is adapted from the Redfield Revisited model, calculated from the *pland* flux and the C:P burial ratio on land:

$$locb = CP_{land} \cdot pland = k_5 \cdot CP'_{land} \cdot pland' \tag{29}$$

The parameter CP_{land} is given the initial baseline value $CP_{land}(0) = 1{,}000$, which LW2 use as representative of lignins. The constant k_5 is defined as present land organic carbon burial rate, with a baseline value of $4.5 \cdot 10^{12}$ mol Cyr^{-1}.

High organic carbon burial has been predicted for the Permo-Carboniferous (for example, Berner and Canfield, 1989; B1; Kump, 1993). Berner and Canfield (1989) and B1 show a high organic carbon burial rate, but do not distinguish land and marine burial. High ocean productivity rates may be postulated to account for this high burial rate, requiring a greater phosphorus input to the oceans, but as the tectonic forcings were not particularly high in this period, this rate would not be sustainable for tens of millions of years. An increase in terrestrial organic carbon burial rates in this period is more consistent with evidence of extensive burial of organic matter in coal swamps (Berner and Canfield, 1989). This increase in burial rate is achieved in COPSE by doubling the C:P burial ratio (CP_{land}) of terrestrially-derived organic matter in the Permo-Carboniferous period.

Ocean Nutrient Model

The ocean nutrient model was taken from the Redfield Revisited models (LW1, LW2) with little change. The model includes marine nitrate and phosphate cycles, new production, and burial of organic matter.

Nitrate and phosphate cycles.—Equations for the following fluxes are detailed in table 5 in appendix 1. Oceanic new production (*newp*) is calculated with both nutrients phosphate and nitrate potentially limiting. Phosphate input to the ocean is determined by phosphate weathering. Bioavailable nitrogen content is increased through nitrogen fixation (*nfix*) and depleted through denitrification (*denit*), keeping nitrate just below its Redfield ratio with phosphate, but making phosphate the ultimate limiting nutrient.

Both nitrogen and phosphorus are buried in organic matter. The phosphorus cycle also includes inorganic burial fluxes, iron-sorbed phosphorus burial (*fepb*) and calcium-bound phosphorus burial (*capb*).

Organic burial.—Marine organic carbon burial (*mocb*) has a quadratic dependency on new production, following LW1:

$$mocb = k_2(newp')^2 \tag{30}$$

where k_2 is present global rate of marine organic carbon burial, and *newp'* normalized new production. Organic **P** and **N** burial fluxes (*mopb* and *monb*) are calculated by the burial ratio of C:N:P in organic matter:

$$monb = mocb \cdot CN_{sea} \tag{31}$$

$$mopb = mocb \cdot CP_{sea} \tag{32}$$

Initial values for the parameters were taken from LW1: $CN_{sea}(0) = 37.5$; $CP_{sea}(0) = 250$. The C:N ratio was not changed, that is, $CN_{sea} = CN_{sea}(0)$ throughout.

Although $CP_{sea} = CP_{sea}(0)$ in the baseline model, an anoxia dependency of this burial ratio was tested as well, following Van Cappellen and Ingall (1994, 1996):

$$CP_{sea} = \frac{k_{oxic} \cdot k_{anoxic}}{(1 - anox) \cdot k_{oxic} + anox \cdot k_{anoxic}} \tag{33}$$

where k_{oxic} and k_{anoxic} are the end-member C:P burial ratios for oxic and anoxic-dysoxic bottom water conditions, respectively, and *anox* is LW1's anoxic fraction of the oceans, which is anti-correlated with both *newp* and atmospheric oxygen. Van Cappellen and Ingall take the end-members to be $k_{oxic} = 200$ and $k_{anoxic} = 4{,}000$. Lenton and Watson (LW1) use this feedback in one version of the Redfield Revisited model, altering the values to $k_{oxic} = 217$ and $k_{anoxic} = 4{,}340$ to keep the present steady state of $CP_{sea}(0) = 250$ and $anox_0 = 0.14$, and these values were adopted for COPSE. This variation of CP_{sea} with the anoxic fraction will be referred to as the 'VCI feedback'.

Marine Sulfur Burial

Sulfate removal from seawater is modeled as two competing processes: (1) as bacterially-mediated reduction followed by sulfide formation and precipitation, most commonly as pyrite, and (2) as non-biological evaporite formation of oxidized sulfur, most commonly as gypsum (Rees, 1970; Kump and Garrels, 1986; Holser and others, 1988). Native sulfur burial and terrestrially-buried sulfur are quantitatively minor (Holser and others, 1988).

Pyrite burial.—The marine pyrite sulfur burial flux *mpsb* is one of the more difficult to quantify, due to the complex relation to organic carbon burial and oxygen levels, besides a sulfate concentration dependency (Holland, 1978; Kump and Garrels, 1986; Holser and others, 1988). The COPSE baseline assumes a dependency on all three factors, with a present value of k_{21}, the same as pyrite weathering, to ensure steady state. A linear dependency on sulfate concentration **S** is assumed for simplicity.

Organic carbon burial dependency of pyrite burial was also explored. Raiswell and Berner (1986) found fairly constant pyrite sulfur / organic carbon ratios in sediment for each geological period, suggesting S_{pyr}:C_{org} = 0.13mol/mol for the Quaternary (last 1.8 million years). This finding is in agreement with the model constants: k_2, the marine organic carbon burial constant was given values of $3.75–4.5 \cdot 10^{12}$ mol Cyr^{-1}, which yields S_{pyr}:C_{org} = 0.12 to 0.14. One option is to assume this constant ratio throughout the Phanerozoic, following Kump and Garrels (1986):

$$mpsb = k_{21} \cdot \mathbf{s} \cdot mocb' \tag{34}$$

where *mocb'* is the normalized marine organic carbon burial flux. This option is also in line with Kump (1993), who proposed a positive relationship between *mpsb* and *mocb*, and a negative one between *mpsb* and *locb* (land-derived organic carbon burial).

However, Raiswell and Berner (1986) show a changing S_{pyr}:C_{org} ratio over the Phanerozoic, being lowest in the Cambrian and Ordovician, rising to a peak in the Permo-Carboniferous, and then dropping to intermediate levels. This sequence is qualitatively similar to proposed pO_2 histories (for example, Berner and Canfield, 1989), and would suggest a dependency of the S_{pyr}:C_{org} ratio on both organic carbon burial rates and oxygen levels.

Petsch and Berner (1998) propose a dependency of pyrite burial on deep ocean anoxia. The COPSE anoxia parameter, taken from LW2, would not provide feedback at high oxygen levels: the anoxic parameter reaches 0, that is, lack of anoxic bottom waters, at pO_2= 1.16 PAL. An inverse dependency on atmospheric oxygen was used

instead, following Berner and Canfield (1989), and providing a stronger oxygen dependency. The full baseline pyrite burial function is therefore:

$$mpsb = k_{21} \cdot \mathbf{s} \cdot \frac{1}{\mathbf{o}} \cdot mocb' \tag{35}$$

Gypsum burial.—The marine gypsum sulfur burial flux *mgsb*, representing gypsum precipitation, is also difficult to estimate. Kump and Garrels (1986) settle for the "unattractive constraint" (*sic*) that the ocean sulfate reservoir is of constant size ($\mathbf{S} = \mathbf{S}_0$). Rees (1970) assumed a constant ratio between ocean sulfate concentration and evaporite formation. This approach was considered better suited to COPSE, despite the irregular occurrences of evaporite precipitating regimes (Holser and others, 1988). Gypsum burial rates were assumed to be linear with sulfate and calcium concentrations, and a burial constant calculated from gypsum weathering rates balancing gypsum burial at present steady state:

$$mgsb = k_{22} \cdot \mathbf{s} \cdot \mathbf{cal} \tag{36}$$

where **cal** is the normalized calcium reservoir. The gypsum burial includes a partial calcium cycle only, which may not accurately represent ocean Ca^{2+} concentration; a more accurate scheme would include Mg^{2+} and $MgSO_4$ burial.

Carbon Isotopes and Fractionation

$\delta^{13}C$ of marine carbonates is predicted in COPSE, rather than the geological record being used as a forcing; this procedure enables comparison of model results to independent geological data. The isotopic composition of each of the carbon reservoirs, **A**, **G** and **C** is tracked. Fractionation is assumed for carbon burial fluxes and biological (productivity) fluxes, and a long-term isotopic equilibrium is assumed between atmosphere and ocean CO_2. These assumptions enable prediction of the $\delta^{13}C$ record, taken to be that of buried carbonates. No fractionation is assumed for weathering and degassing fluxes.

Atmosphere-ocean fractionation.—Mook (1986) gives the equilibrium between atmospheric CO_2 and dissolved bicarbonate as:

$$^{13}\varepsilon[CO_2(gas) - HCO_3^-(aq)] = -9483/T_k + 23.89‰ \tag{37}$$

where T_k is temperature in Kelvin. We approximate the isotopic composition of bicarbonate for that of ΣCO_2 (total dissolved CO_2):

$$\delta_a = \delta_o - 9483/T_k + 23.89‰ \tag{38}$$

where δ_a is $\delta^{13}C$ of atmospheric CO_2, and δ_o that of ocean δCO_2. Isotopic mass balance yields:

$$\delta_a \cdot \varphi \cdot \mathbf{A} + \delta_o(1 - \varphi)\mathbf{A} = \delta_A\mathbf{A} \tag{39}$$

where $\delta_\mathbf{A}$ is the isotopic composition of **A**, and φ the atmospheric fraction of **A**. The baseline model assumes a constant atmospheric fraction, 0.01614, calculated from a pre-industrial pCO_2 of 280 ppm. Solving the simultaneous equations yields:

$$\delta_o = \delta_A + \varphi(9483/T_k - 23.89‰) \tag{40}$$

$$\delta_a = \delta_A + (\varphi - 1)(9483/T_k - 23.89‰) \tag{41}$$

Marine carbonate carbon fractionation.—Sedimentation and dissolution of calcium carbonate in the ocean results in temperature dependent carbon isotope fraction-

ation. The equilibrium fractionation factor for calcite and dissolved inorganic carbon was taken from Mook (1986):

$$^{13}\varepsilon[CaCO_3(calc) - HCO_3^-(aq)] = -4232/T_k + 15.10‰ \quad (42)$$

Approximating δ_o for bicarbonate isotopic composition, and calcite burial for total marine carbonate carbon burial (*mccb*), yields a flux fractionation of:

$$\delta_{mccb} = \delta_o + 15.10‰ - 4232/T_k \quad (43)$$

An aragonite sedimenting ocean would show stronger fractionation. Assuming equal temperature dependency to calcite, the flux fractionation would be (Mook, 1986):

$$\delta_{mccb} = \delta_o + 16.90‰ - 4232/T_k \quad (44)$$

or a 1.8 permil increase in $\delta^{13}C$ over the value for calcite.

The geological $\delta^{13}C$ record refers to the $\delta^{13}C$ of sedimented carbonates; hence the model prediction of δ_{mccb} is the $\delta^{13}C$ parameter, which will be compared to paleodata.

Marine organic carbon fractionation.—The isotopic composition of buried marine organic carbon is often calculated using a fractionation factor between carbonate and organic matter being buried (for example, Derry and France-Lanord, 1996; Raymo, 1997; Hayes and others, 1999). Following Hayes and others (1989), this factor can be expressed as:

$$\delta_{mocb} = \delta_{mccb} - \Delta_B \quad (45)$$

where δ_{mocb} is the isotopic composition of buried marine organic carbon (*mocb*), and Δ_B is the mean isotope fractionation between carbonate and organic carbon burial. *In our notation*, Δ_B is defined as positive, that is, 'stronger' fractionation = larger Δ_B, resulting in marine organic sediment with a lower (more negative) $\delta^{13}C$. The same approach is used with Δ_P, the fractionation in the burial of terrestrially-derived organic matter, and with Δ_S, the $\delta^{34}S$ fractionation of marine pyrite sulfur burial.

The compiled data of Hayes and others (1999) give values of 28 to 32 permil for most of the Phanerozoic, reflecting "maximal fractionation of carbon isotopes by phytoplanktonic producers", and a nearly linear decline from 30 permil in the Early Oligocene (~30MaBP) to 22 permil at present, due partly to low pCO_2 levels. Raymo (1997) also suggests a drop in Δ_B from 60MaBP onwards, most likely driven by low pCO_2. She considers values of ~24 to 28 permil of the past 40MaBP, decreasing stepwise or gradually. Derry and France-Lanord (1996), in a study of the Neogene (past 24MaBP), take Δ_B to be 24.5 permil up to 7MaBP, then dropping to 23.5 permil.

Changes in Δ_B dependent on pCO_2 and pO_2 are considered, and the general fractionation is thus expressed as:

$$\Delta_B = \Delta_B^0 + \varepsilon_B(CO_2) + \varepsilon(O_2) \quad (46)$$

where $\varepsilon_B(CO_2)$ and $\varepsilon(O_2)$ are the fractionation effects of changing pCO_2 and pO_2 levels, and $\Delta_B^0 = 33$ permil is an imposed upper limit of fractionation.

Δ_B is taken to be 24 permil at present. Assuming pCO_2 levels to be the major source of variation, we attempt to mathematically capture Phanerozoic Δ_B values using the following formula:

$$\varepsilon_B(CO_2) = \frac{-9}{\sqrt{\mathbf{a}}} \quad (47)$$

where **a** is normalized atmosphere-ocean CO_2. This equation yields 27.8 permil at pCO_2 = 3PAL, rising to 29 permil at 5PAL and 31 permil at 20PAL. Model predictions see pCO_2 drop almost continuously from ~120MaBP onwards, dropping below 3PAL only in the past ~40 million years. Equation (47) thus ensures that for most of the Phanerozoic Δ_B values are above 28 permil, and drop towards 24 permil during the Paleogene (past 65 million years), in agreement with Raymo (1997) and Hayes and others (1999).

High atmospheric oxygen levels may increase the carbon isotope fractionation by vascular land plants and marine plankton, as seen in experiment and incorporated in models (Berner and others, 2000; Beerling and others, 2002). Berner and others (2000) suggested a linear relationship:

$$\varepsilon(O_2) = J(\mathbf{o} - 1) \tag{48}$$

where **o** is normalized pO_2 and J is a curve fit parameter. The COPSE baseline uses their best fit value of $J = 5$.

A strong pO_2 effect on fractionation would lead to lower (that is, more negative) organic matter $\delta^{13}C$ when pO_2 is high. Thus in the Permo-Carboniferous, when both pO_2 and organic carbon burial are believed to be high, $\varepsilon(O_2)$ is expected to leave atmosphere-ocean $\delta^{13}C$ (and hence the marine carbonate $\delta^{13}C$ record) more positive, in agreement with records.

Land plant fractionation.—Land plant fractionation Δ_P is expressed as the fractionation between atmospheric CO_2 and plant material. No additional fractionation was assumed between land plant matter and land-derived buried organic carbon. Δ_P is expressed similarly to that of marine organic carbon burial:

$$\Delta_P = \Delta_P^0 + \varepsilon(O_2) \tag{49}$$

where the oxygen dependency $\varepsilon(O_2)$ is the same as that of marine plankton. The present fractionation value was taken as Δ_P = 19 permil, following Popp and others (1989). The effect of varying fractionation with pCO_2 levels (following Farquhar and others, 1982) was found to be very small, and was not included in the baseline model.

Sulfur Isotopes and Fractionation

The isotopic composition of each of the sulfur reservoirs, **S**, **GYP** and **PYR** is tracked, enabling COPSE to predict the $\delta^{34}S$ record of evaporite sulfur (gypsum) for further comparison to geological data. As with carbon, sulfur weathering processes are assumed not to fractionate. Holser and others (1988) estimate sulfate deposition has a fractionation factor of 1.0 to 1.6 permil, much smaller than that of pyrite burial. Many sulfur cycle modeling papers (for example, Kump and Garrels, 1986; Kump, 1993; Petsch and Berner, 1998) assume fractionation for pyrite burial, but not for gypsum burial, and this approach was taken with COPSE.

Marine burial of pyrite sulfur (*mpsb*) involves biological reduction of sulfate. Bacteriogenic sulfides, generalized here as pyrite, show a marked bias in favor of the lighter ^{32}S isotope. The range of fractionation is quite large, 30 to 45 permil (Holser and others, 1988). It is convenient to define the fractionation factor between the ocean sulfate and the buried pyrite (sulfide):

$$\Delta_S = \delta^{34}S_{sulfate} - \delta^{34}S_{sulfide} \tag{50}$$

Modeling papers often take the fractionation factor as a constant Δ_S = 35 permil (Garrels and Lerman, 1984; Kump and Garrels, 1986; Petsch and Berner, 1998). This value was used in the COPSE baseline.

TABLE 3

COPSE model runs in this paper. Description shows how various runs differ from the baseline. Runs 10–12 differ from the baseline only in isotope fractionation, with mass fluxes unchanged, that is, runs 10 and 11 are identical to the baseline except for the $\delta^{13}C$ *prediction, and run 12 except for the* $\delta^{34}S$ *prediction.*

Run no.	Description
1	Baseline
2	Marine organic C:P burial ratio is anoxia-dependent, using (33)
3	Oxidative weathering *not* dependent on pO_2: (22) replaces (21)
4	'Friend' feedback used for V (terrestrial vegetation): (53) replaces (5)
5	Temperature independent 'Friend' feedback used for V: (53) replaces (5)
6	Strong fire feedback: $k_{fire} = 20$ in (8)
7	No fire feedback: (9) replaces (8)
8	Pyrite burial *not* dependent on pO_2: (34) replaces (35)
9	No sulfur cycle (all sulfur reservoirs and fluxes set to 0)
10	Aragonite burial: during 'aragonite sea' periods, (44) replaces (43)
11	$\delta^{13}C$ fractionation *not* dependent on pO_2: $\varepsilon(O_2) = 0$ in (46)
12	$\delta^{34}S$ fractionation dependent on pO_2: (51) used rather than constant Δ_S

An alternative fractionation with a linear pO_2 dependency was tested as well, following Berner and others (2000). They reasoned that S cycling in sediments is O_2 dependent, and that more recycling increases ^{34}S depletion, leading to:

$$\Delta_S = 35‰ \cdot \mathbf{o} \tag{51}$$

RESULTS

We present results for the baseline COPSE model and for variants of the model using alternative flux functions described in the previous section. Twelve different runs are presented, as described in table 3.

Phanerozoic pO_2

Figure 3A shows Phanerozoic oxygen predictions of several COPSE model runs, compared with an existing model prediction, and with constraints suggested by the pO_2 requirement of the Cambrian fauna and from a further model. Figure 3C shows the effect of varying the strength of the fire feedback on pO_2 from 350 MaBP to present. The continuous records of charcoal and of forests over the last 350 Ma set lower and upper limits on pO_2, respectively, but the tightness of these pO_2 constraints is debated.

The baseline COPSE model prediction (run 1) has Early Paleozoic pO_2 ~0.25 PAL, lower than the pO_2 ~0.6 PAL suggested by the Lasaga and Ohmoto (2002) model, but well above the pO_2 ~0.1 PAL required by the Cambrian fauna (Holland, 1984). The rise of land plants brings about a rise in pO_2, consistent with the

appearance of the first fossil charcoal ~370 MaBP (Cressler, 2001). From ~350 MaBP onwards, oxygen is regulated in the range pO_2 ~1 to 1.5 PAL and is slightly overestimated at 1.08 PAL at present. There are two O_2 peaks in the Permo-Carboniferous and the Cretaceous. The Permo-Carboniferous peak of pO_2 ~1.4 PAL is the result of land plants colonizing the continents, with high burial rates of terrestrially derived organic carbon accentuated by an imposed doubling of CP_{land}. The Cretaceous peak of pO_2 ~1.55 PAL is due to a combination of high degassing rates and the evolution of angiosperms. Increased CO_2 input from degassing drives up CO_2 concentration resulting in increases in silicate and phosphorus weathering rates. The greater weathering flux of phosphorus results in greater marine productivity and increased organic carbon burial on both land and sea, in turn raising pO_2 levels. High pO_2 levels suppress vegetation biomass, which should drive down weathering rates, closing a negative feedback loop; however, the rise of angiosperms counteracts this relationship by increasing the weathering amplification by land plants. Both oxygen peaks exceed 1.25 PAL or 25 volume percent mixing ratio (assuming a constant N_2 reservoir), which is the most stringent upper limit for the persistence of forests quoted in the literature (for example LW2). However, the oxygen peaks lie below a more conservative upper limit of 1.6 PAL or 30 volume percent mixing ratio (Watson, ms, 1978).

The alternative model runs show the effects of different feedbacks on atmospheric oxygen. In run 2 (fig. 3A) we add the VCI negative feedback on pO_2 in which the C:P burial ratio of marine organic matter increases markedly under anoxic conditions. In the early Paleozoic, pO_2 is increased to 0.5 to 0.6 PAL, the VCI feedback having a dominant effect over other O_2 feedbacks. However, after the advent of land plants, higher pO_2 levels result in anoxia disappearing from the oceans, so that the regulatory effect of the VCI feedback disappears between 300 to 200 MaBP. After 200 MaBP the VCI feedback has a minor effect of lowering O_2 concentration.

In run 3, the pO_2 dependency of oxidative weathering of reduced carbon and sulfur is removed. The removal of this feedback results in extremely low $pO_2 < 0.05$ PAL in the early Paleozoic, because lower pO_2 no longer reduces the oxygen sink. Predicted pO_2 is less than the estimated requirements of Cambrian fauna, suggesting that additional negative feedback on pO_2 existed at the time, be that the oxidative weathering feedback or something else. Combining runs 2 and 3, that is, adding the VCI feedback and removing pO_2 dependency of oxidative weathering (not shown) resulted in pO_2 qualitatively similar to run 2, with early Paleozoic pO_2 of 0.4 to 0.5 PAL and the two peaks somewhat higher than the baseline.

In run 9 (fig. 3A) the sulfur cycle is entirely removed from the baseline model, losing the ability to 'shuttle' oxygen between C and S reservoirs. Early Paleozoic $pO_2 <$ 0.1 PAL is again inconsistent with the estimated requirements of Cambrian fauna. Furthermore, after the advent of land plants, pO_2 peaks at >1.6 PAL in the Permo-Carboniferous, and remains >1.1 PAL to the present. The results for run 8 (not shown) in which the sulfur cycle is included but the inverse dependency of pyrite burial on oxygen, which serves as a negative feedback, is removed show the same qualitative changes as run 9. These runs suggest that the sulfur cycle, in particular an inverse dependency of pyrite burial on oxygen, has played an important role in reducing atmospheric oxygen variations over Phanerozoic time.

Figure 3B compares the different calculations of terrestrial vegetation *V*. The baseline uses the OCT feedback, whereas runs 4 and 5 use the Friend feedback. The pO_2 predictions are similar for most of the Phanerozoic, but high temperatures in the Cretaceous and Cenozoic result in high productivity on land in run 4, which in turn yield unrealistically high pO_2 levels, up to 2 PAL. The Friend feedback is based on modeling leaf photosynthesis, and may overestimate the effect of temperature on global productivity: a drop in *T* from 20°C to 15°C results in a 28 percent drop in *V* at

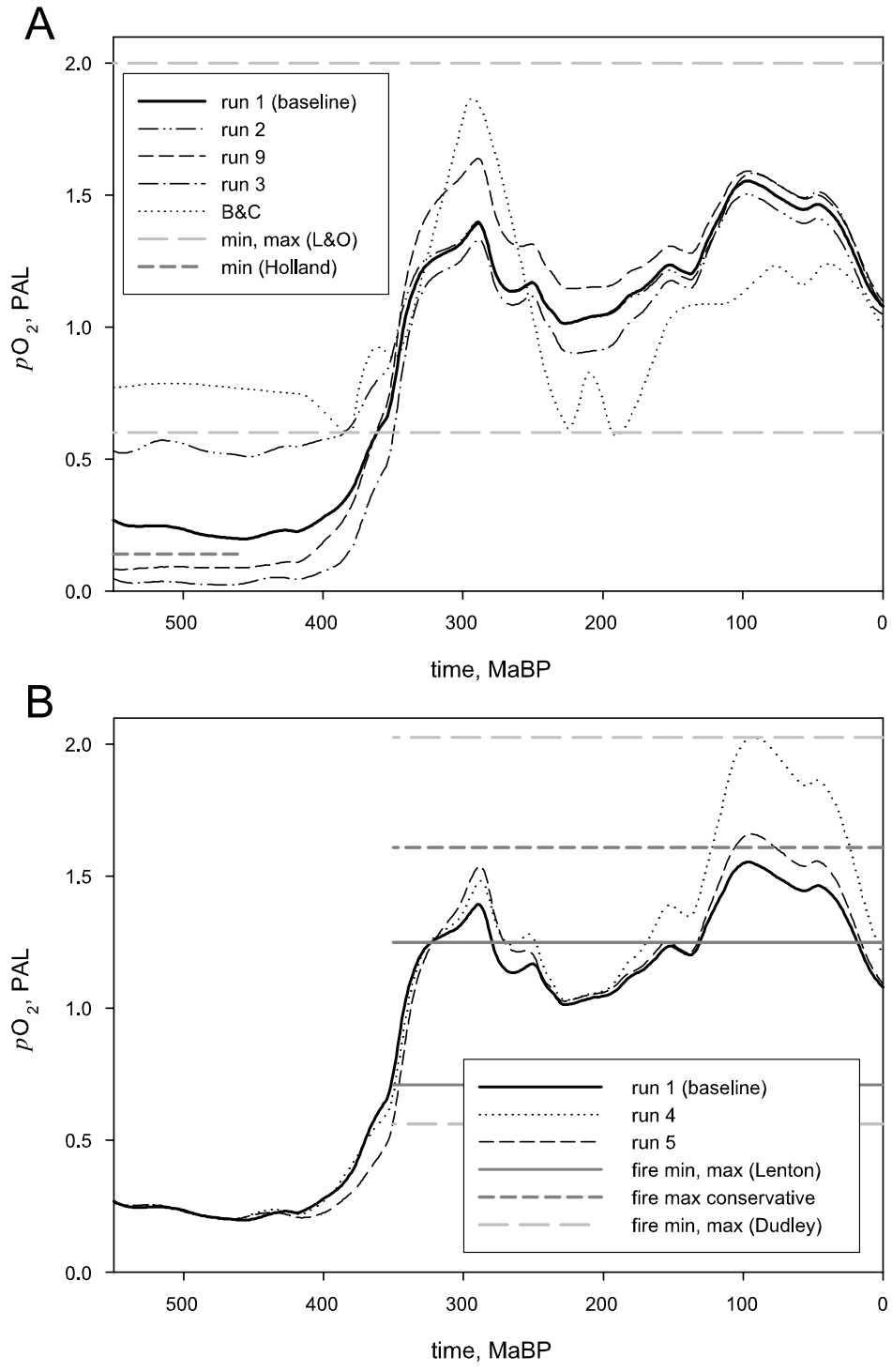
A
2.0
1.5
1.0
0.5
0.0
pO_2, PAL
run 1 (baseline)
run 2
run 9
run 3
B&C
min, max (L&O)
min (Holland)
500
400
300
200
100
0
time, MaBP
B
2.0
1.5
1.0
0.5
0.0
pO_2, PAL
run 1 (baseline)
run 4
run 5
fire min, max (Lenton)
fire max conservative
fire min, max (Dudley)
500
400
300
200
100
0
time, MaBP

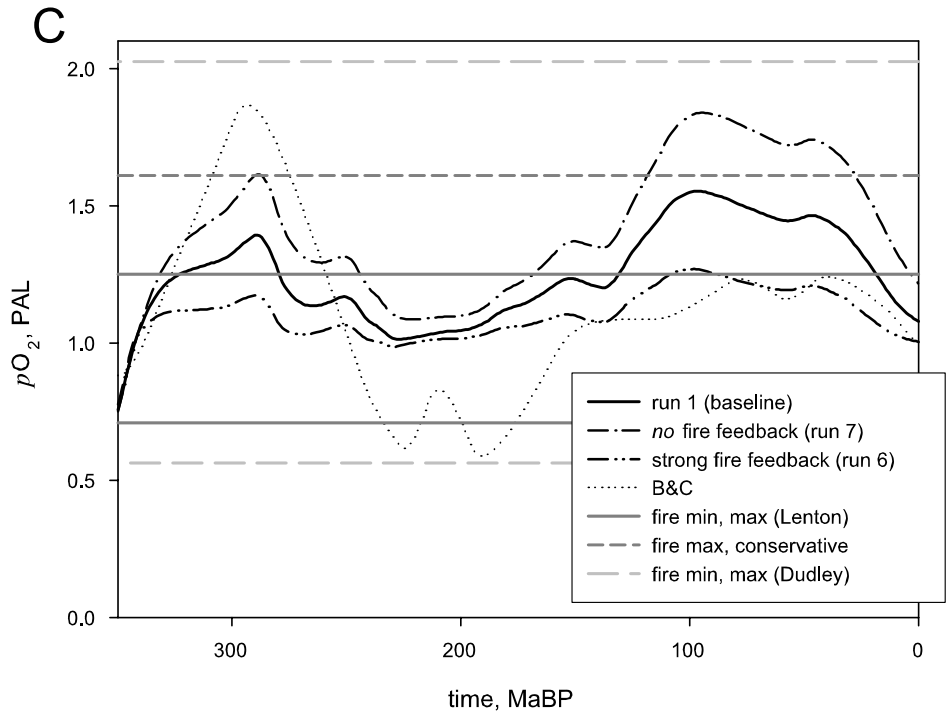

Fig. 3. A compilation of Phanerozoic pO_2 predictions and constraints, as compared with COPSE predictions. Straight lines below PAL are suggested minima and above it, suggested maxima. (A) Model runs 1 (baseline), 2 (VCI feedback), 3 (no oxidative weathering feedback) and 9 (no S cycle) are compared with Phanerozoic pO_2 model prediction by Berner and Canfield (1989) — dotted line marked B&C; constraints suggested by Lasaga and Ohmoto (2002) — light dashed lines — L&O; and suggested minimum pO_2 for Cambrian fauna (Holland, 1984) – dark dashed line. (B) Model baseline (run 1), which uses the 'OCT' feedback for terrestrial vegetation *V* is compared to predictions using the full 'Friend' feedback (run 4) and the temperature independent version (run 5). Also shown are charcoal record constraint for minimal pO_2 allowing combustion and maximal pO_2 allowing forest regeneration from fires (Lenton, 2001) – dark gray lines; a more liberal maximum for forest fires – dashed dark gray line; and charcoal record constraints as interpreted by Dudley (2000) – light gray dashed lines. (C) The effect of the fire feedback on pO_2 predictions from 350 MaBP to present is tested by comparing COPSE runs 1 (baseline), 6 (stronger fire feedback) and 7 (no fire feedback).

current pO_2 and pCO_2 levels, and more than 40 percent at high pCO_2 levels, while a similar cooling would result in a drop of only 12.5 percent in *V* using the OCT feedback. Run 5 checks the effect of removing the direct *T* effect in the Friend feedback (see appendix 2), resulting in a prediction of pO_2 (and other parameters, not shown) very similar to the baseline. This result implies that strong O_2 and CO_2 feedbacks on V are more important than the exact functions used.

In runs 6 and 7 (fig. 3C) the fire feedback is varied from the baseline. Strengthening the fire feedback as in LW2 (run 6) results in tighter pO_2 regulation, with peaks of 1.17 PAL in the Permo-Carboniferous and 1.27 PAL in the Cretaceous. These values nearly meet the stringent constraint of 1.25 PAL (25 vol%) from LW2. Furthermore, pO_2 returns to 1.0 PAL at present. Removing the fire feedback entirely (run 7) results in pO_2 being poorly regulated after land plants become established, rising to ~1.6 PAL in the Permo-Carboniferous and ~1.85 PAL in the Cretaceous, and only dropping to 1.22 PAL at present. These results suggest that some degree of fire feedback has stabilized atmospheric oxygen over the past 350 Ma.

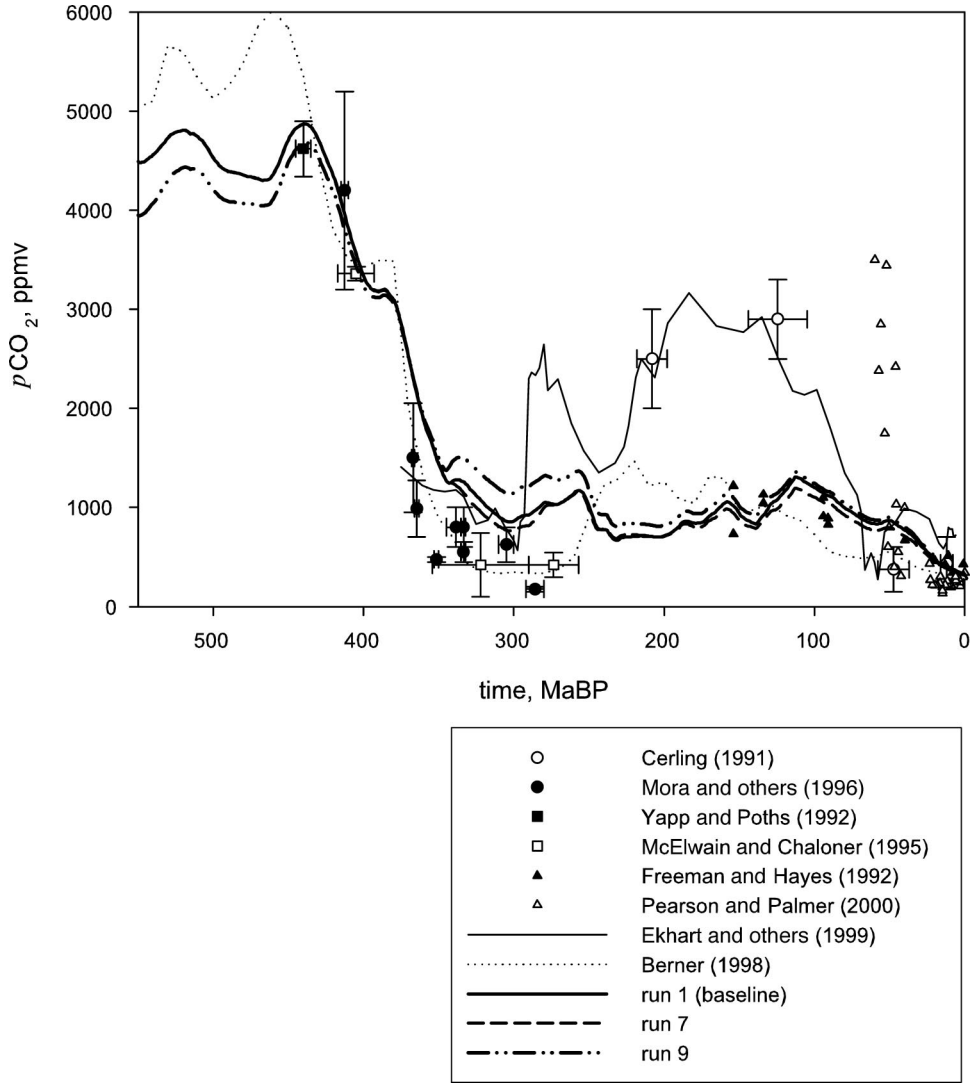

Fig. 4. Phanerozoic pCO_2 predictions of the COPSE model runs 1 (baseline), 7 (no fire feedback) and 9 (no S cycle) compared to a compilation of proxies and models, with PAL taken to be 280 ppm. Data include Berner (1998) in a version of the Geocarb model; Proxies are from Cerling (1991); Freeman and Hayes (1992); Yapp and Poths (1992); McElwain and Chaloner (1995); Mora and others (1996); Ekart and others (1999); Pearson and Palmer (2000).

Phanerozoic pCO_2 and Temperature

Figure 4 shows Phanerozoic pCO_2 predictions of variants of the COPSE model compared with a range of proxies and an alternative model prediction. The baseline model (run 1) has pCO_2 ~14 to 18 PAL in the Early Paleozoic, followed by an order of magnitude drop to a Permo-Carboniferous minimum of ~3.0 PAL at ~300 Ma. From then on pCO_2 is regulated in the range 1 to 5 PAL. There is a broad minimum in the Triassic, a gentle rise to a peak in the Cretaceous and a decline in the past 100 million years. The COPSE model predictions are in fair agreement with pCO_2 proxies, bearing

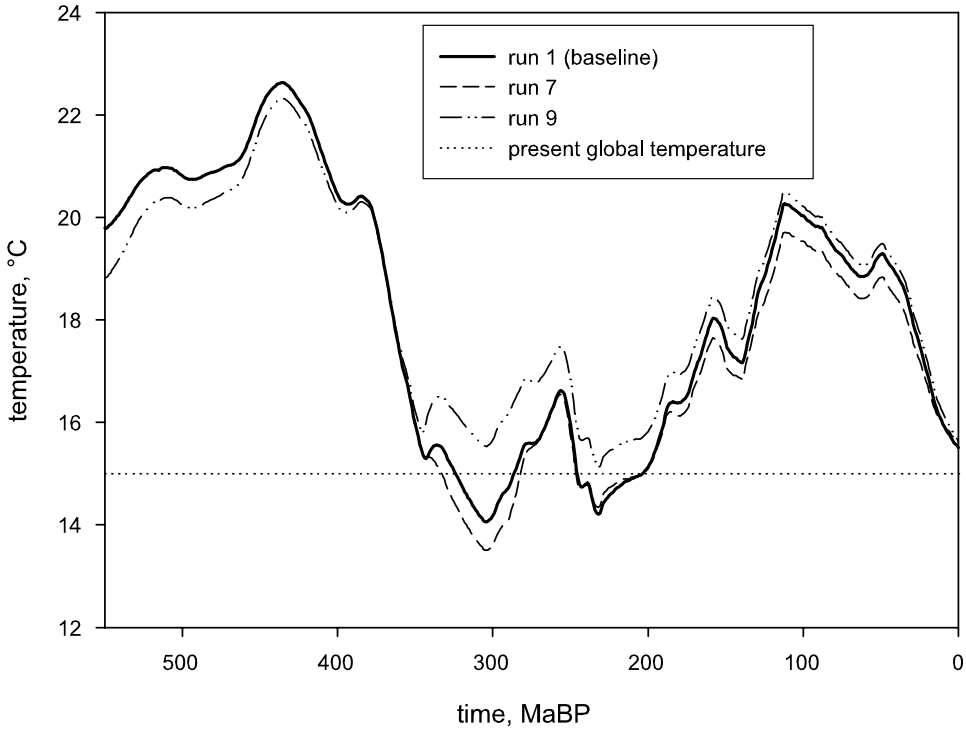

Fig. 5. Phanerozoic temperature predictions of three COPSE model runs, baseline (run 1), no fire feedback (run 7) and no S cycle (run 9).

in mind that there are large discrepancies between the different proxies in some intervals. The Devonian fall of pCO_2 is not rapid enough and the minimum pCO_2 predicted in the Permo-Carboniferous is not as low as most proxies. The prolonged Mesozoic peak that some proxies show is missing. The trend over the last 150 Ma is in good agreement with one proxy (Freeman and Hayes, 1992) but not others.

Temperature predictions of COPSE (fig. 5) necessarily follow trends similar to pCO_2, due to the calculation of T from pCO_2 and insolation. The predictions are at best semi-quantitative, as they do not account for the climatic effects of factors such as changing continental configuration. The general trend is of a warm Early Paleozoic, dropping to a cold Permo-Carboniferous and Triassic, rising to a warm Cretaceous, and then cooling until the present. The baseline predicts a Permo-Carboniferous trough with a minimum 1.4°C colder than present, consistent with the occurrence of glaciations in the Permo-Carboniferous period. However, the earlier, short Ordovician glaciation is not captured.

The predictions of pCO_2 (fig. 4) and temperature (fig. 5) proved robust in the face of changes in the model flux functions, but more sensitive to changes in the historical forcing functions. Removing the much-debated fire feedback (run 7) has a surprisingly small effect on pCO_2 predictions, lowering the Permo-Carboniferous minimum to pCO_2 ~2.7 PAL and reducing pCO_2 slightly throughout the last ~190 Ma. Temperatures reach a lower Permo-Carboniferous minimum 2°C below present, and the Cretaceous is slightly less warm. In contrast, the removal of the sulfur cycle from the model (run 9) raises pCO_2 in the Carboniferous, Permian and Triassic giving minimum Permo-Carboniferous pCO_2 ~4.0 PAL. Removing the sulfur cycle results in

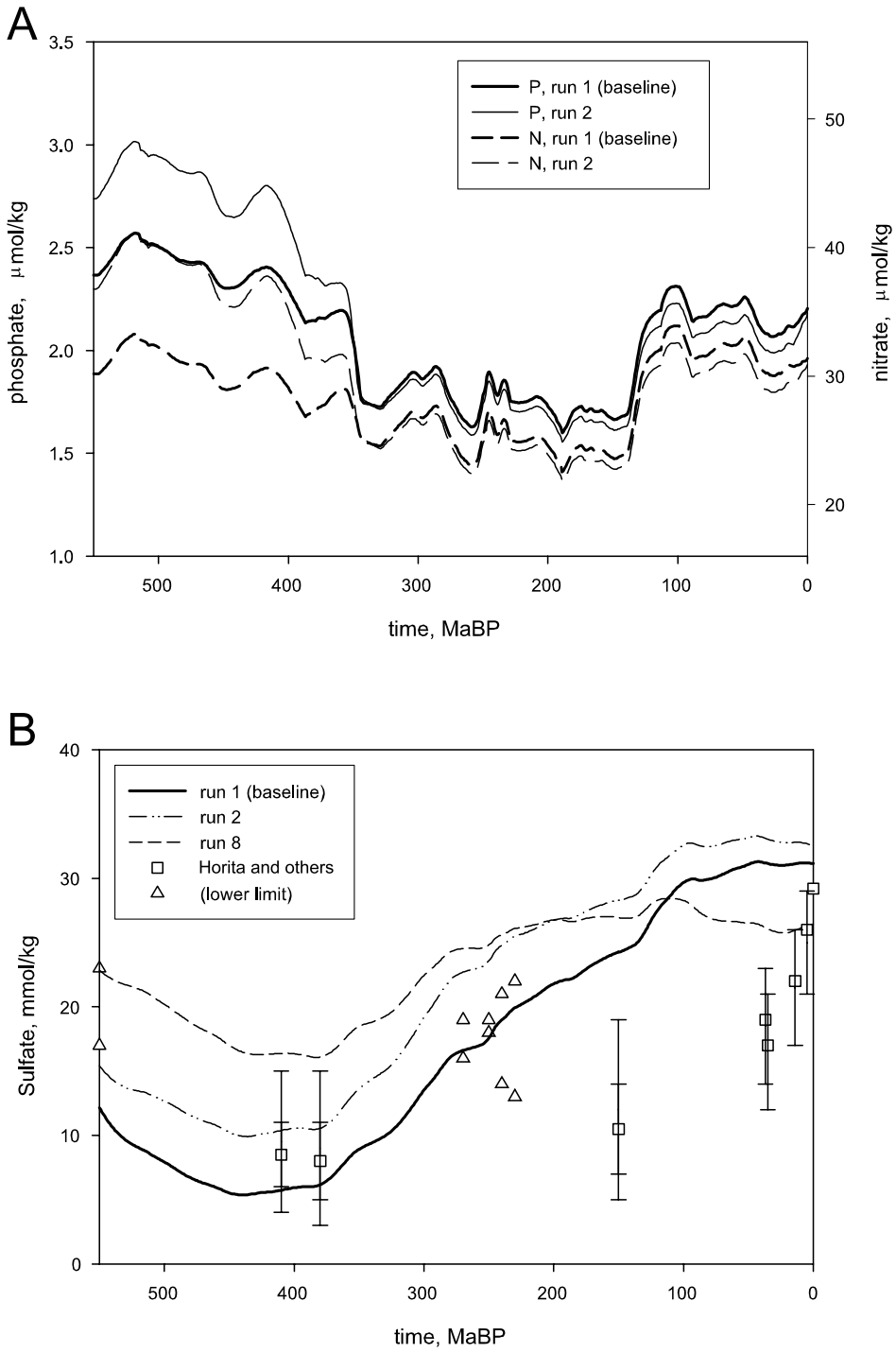

Fig. 6. COPSE prediction of ocean parameters (A) phosphate and nitrate, (B) sulfate and (C) calcium, for the baseline (run 1), run 2, and (in B and C only) run 8. Run 2 includes the VCI feedback, and in run 8 pyrite burial dependency on pO_2 is removed.

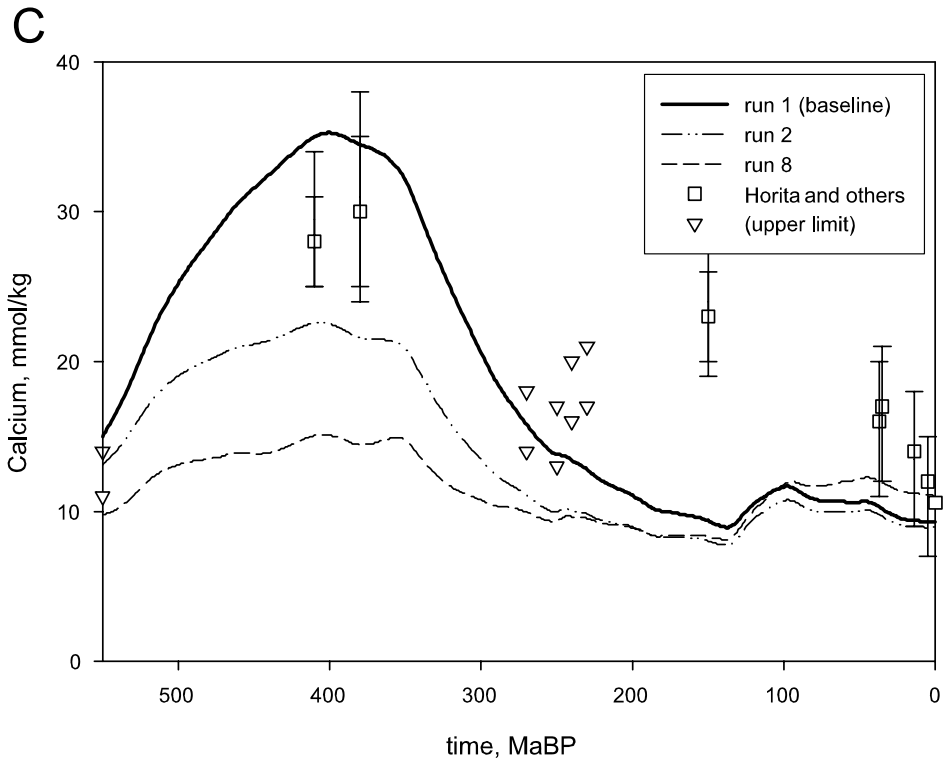

Fig. 6. (continued)

temperatures above present throughout the Phanerozoic, including the Permo-Carboniferous, and is at odds with evidence of Permo-Carboniferous glaciations. This result indicates an important influence of the S cycle on CO_2 as well as O_2 over Phanerozoic time.

Ocean Composition

The COPSE representation of ocean composition is rather simple, but nonetheless the history of some ocean parameters is worth exploring and comparing to data. Figure 6A shows ocean phosphate and nitrate for the baseline run 1 and for the inclusion of the VCI feedback (run 2). Figure 6B shows ocean sulfate and figure 6C ocean calcium, for runs 1 and 2 and for the removal of the pyrite burial feedback (run 8).

Phosphate is predicted to be above present concentration in the Early Paleozoic, dropping to below present concentration in the Carboniferous through to the Jurassic, and rising to near present levels from the Cretaceous onwards. With the VCI feedback included (run 2) phosphate concentration is raised in the early Paleozoic due to preferential phosphorus recycling under anoxic conditions manifest in the higher marine organic C:P burial ratio. The COPSE prediction of phosphate variation is in fair agreement with Guidry and Mackenzie (2000), who present a global P cycle model based on apatite weathering. They predict elevated P weathering and transport in the Paleozoic, resulting in higher new production in the oceans, and a general decrease in the phosphorus flux to the oceans from the Early to the Late Phanerozoic.

Nitrate is regulated below Redfield ratio to phosphate throughout the Phanerozoic. In the baseline model, the deviation from Redfield ratio is greatest in the Early Paleozoic due to low pO_2, increased ocean anoxia and increased denitrification. Including the VCI feedback raises Early Paleozoic pO_2 and brings nitrate closer to Redfield ratio to phosphate.

Oceanic sulfate is predicted to be less than half of present ocean concentration in the Early Paleozoic, rising from the Carboniferous through the Cretaceous, when it reaches near present concentration. In a study of Phanerozoic seawater changes, Hardie (1996) predicts much smaller changes in ocean sulfate, with Paleozoic levels ~ 15 percent lower than present. However, in a recent study of Silurian seawater composition, Brennan and Lowenstein (2002) estimate Silurian sulfate concentration to be much lower than present, with a best fit of $[SO_4^{=}] = 11$ mmolal, or 0.38 of present concentration (29 mmolal), similar to the baseline model predictions.

Calcium concentration in the baseline model is predicted to be high in the Early Paleozoic, reaching a peak of 2 to 3.5 times present concentrations ca. 400 MaBP, and dropping to near present concentration in the Permian. This concentration range agrees with Stanley and Hardie (1998), who predict $[Ca^{2+}]$ concentration ~2.5 times present in the Early Paleozoic, but their second peak of ~3 times present in the Cretaceous is lacking. The VCI feedback lowers the $[Ca^{2+}]$ peak to ~2 times present. Removing the pyrite burial feedback even more markedly dampens $[Ca^{2+}]$ variation. These effects can be understood in terms of changes in gypsum burial, which removes Ca^{2+}. In the baseline model, low pO_2 in the Early Paleozoic increases pyrite burial, and gypsum burial must be correspondingly suppressed to balance the sulfate budget, thus giving higher than present $[Ca^{2+}]$. With the VCI feedback, Early Paleozoic pO_2 is increased, pyrite burial is less enhanced, gypsum burial less suppressed, and the increase in $[Ca^{2+}]$ consequently smaller. Without the inverse relationship between pO_2 and pyrite burial, pyrite and gypsum burial are more similar to present in the Early Paleozoic, giving rise to similar $[Ca^{2+}]$.

Organic Carbon Burial

Figure 7A shows predicted total organic carbon burial flux over the Phanerozoic. The present burial rate was taken to be $9 \cdot 10^{12}$ mol C yr^{-1}, divided evenly between terrestrial and marine derived carbon. Most sources estimate a lower percentage of terrestrially derived organic carbon burial, but some give 50 percent as an upper limit (Kump, 1993, LW2). Our baseline burial rate and percentage from land were chosen to give the best oxygen regulation. The baseline run shows a very similar trend in the Paleozoic to the predictions of Berner and Canfield (1989) based on the data of Ronov (1976), with a significant increase in burial rates with the advent of land plants. However, Mesozoic and Cenozoic carbon burial rates are higher in COPSE, with the present rate similar to the Permo-Carboniferous maximum. In contrast, Berner and Canfield (1989) assume a present burial rate of only $5 \cdot 10^{12}$ mol C yr^{-1}.

Including an increase in marine organic C:P burial ratio (CP_{sea}) at low pO_2 levels (the VCI feedback: run 2, fig. 7A) generates higher burial rates in the Early Paleozoic. This result may under-predict the increase in organic C burial when land productivity rose (Berner and Canfield, 1989; Kump, 1993). Removing the fire feedback (run 7, fig. 7A) slightly increases burial rates after the advent of land plants, without changing the overall trend.

Figure 7B shows the division between terrestrial and marine derived organic carbon burial in the baseline run. Marine burial is dominant until the Permo-Carboniferous, when there is a massive pulse of carbon burial on land, in line with other predictions (Kump, 1993); the reader is reminded that the increase of carbon burial on land was artificially created in COPSE by doubling the C:P burial ratio of terrestrially derived organic matter in this period. The burial flux of terrestrially

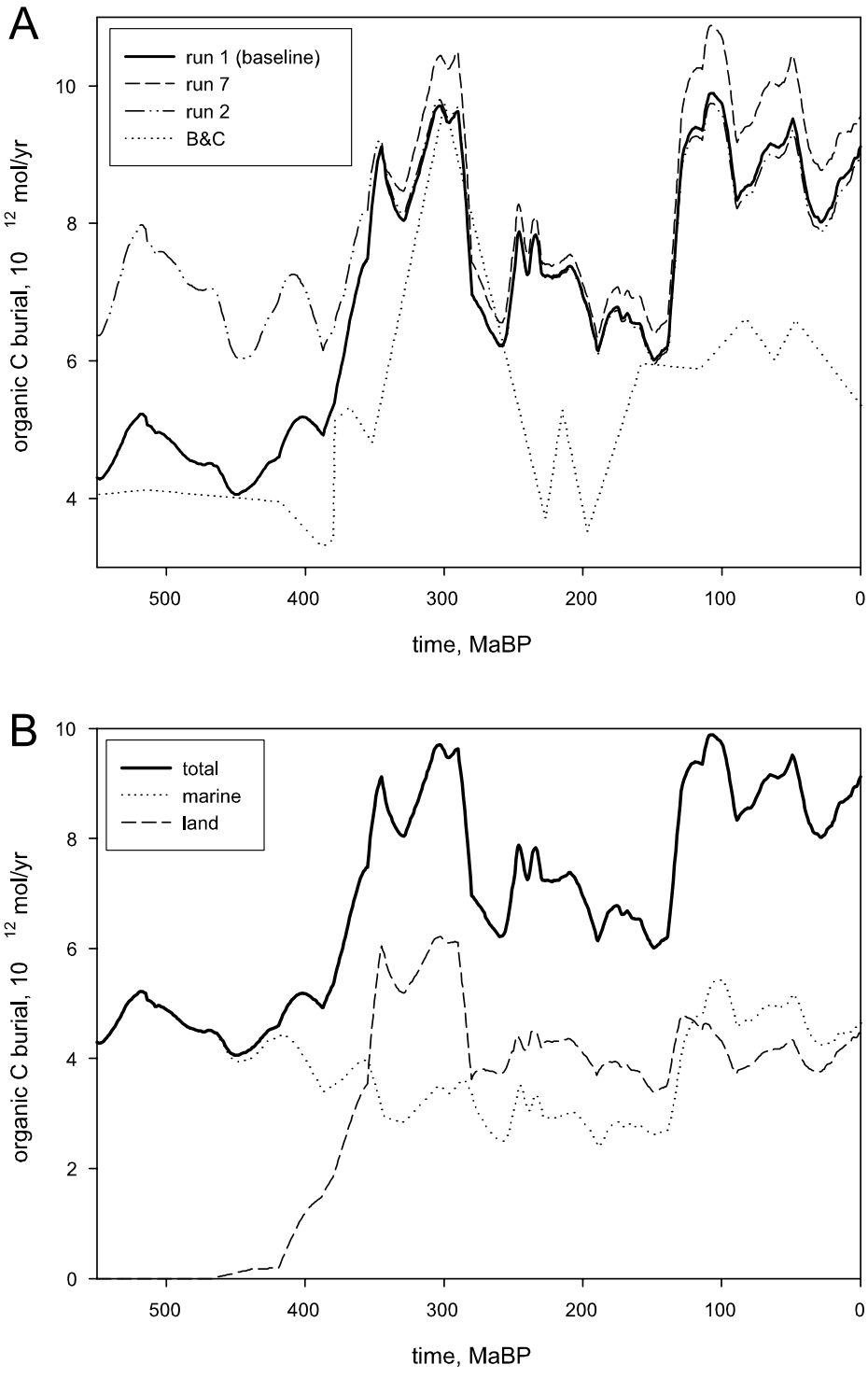

Fig. 7. Organic carbon burial predictions. Present burial rate is taken to be $9 \cdot 10^{12}$ mol C yr^{-1}, divided evenly between terrestrial and marine derived carbon. (A) Total organic C burial for COPSE runs 1 (baseline), run 2 (VCI feedback), and run 7 (no fire feedback), with dotted line marked B&C — the prediction of Berner and Canfield (1989) for comparison. (B) The division in the baseline model of organic carbon burial between terrestrial and marine origin.

derived organic matter exceeds that of marine organic matter until the Cretaceous. Then increased degassing rates, pCO_2 and temperature, followed by the rise of angiosperms, result in an increased phosphorus weathering flux to the sea that increases marine productivity and organic carbon burial. Land productivity increases initially but is then suppressed as pO_2 levels rise.

Phanerozoic $\delta^{13}C$

Figure 8 shows Phanerozoic $\delta^{13}C$ predictions of several COPSE model runs, including a comparison to the record of Veizer and others (1999) in figure 8A. The baseline (run 1) gives a better $\delta^{13}C$ prediction than most of the other runs. Although the overall similarity in trend is encouraging, there are three major differences between model predictions and the $\delta^{13}C$ record. First and foremost, the amplitude of $\delta^{13}C$ increase from the Early Paleozoic to the Permo-Carboniferous is too small. Second, the Devonian peak in the $\delta^{13}C$ record is missing, which may indicate that early land plant evolution is not being properly captured. Finally, the Late Paleozoic – Early Mesozoic peak ends too soon, with predicted Late Carboniferous and Permian $\delta^{13}C$ values lower than the record values. This discrepancy may be due to the forced increase in Carboniferous land-derived organic carbon burial insufficiently capturing Earth system changes.

Varying O_2 feedbacks has a significant effect on Early Paleozoic $\delta^{13}C$ prediction (fig. 8A). Including the VCI feedback (run 2), results in Cambrian and Ordovician $\delta^{13}C$ higher than the record, because higher pO_2 results in stronger carbon isotope fractionation. The overall amplitude of change is also too small. Removing the pO_2 dependency of oxidative weathering (run 3), lowers early $\delta^{13}C$ more than any other record, because lower pO_2 results in reduced biological carbon isotope fractionation. Combining the two runs — that is, including the VCI feedback and removing pO_2 dependency of oxidative weathering — (not shown) resulted in a prediction similar to run 2, slightly closer to the baseline, but with early Paleozoic $\delta^{13}C$ still higher than the record.

The fire feedback (fig. 8B) affects $\delta^{13}C$ after the establishment of land plants, especially in the Permo-Carboniferous and the Cretaceous. Strengthening the fire feedback (run 6) worsens the $\delta^{13}C$ prediction, as the Permo-Carboniferous high is not sustained. Removing the fire feedback (run 7) improves the Permo-Carboniferous prediction, but $\delta^{13}C$ still falls too soon, and then the Mesozoic maximum strays higher than the record.

Changes to the sulfur cycle (fig. 8C) primarily affect Early Paleozoic $\delta^{13}C$. Removing the inverse dependency of pyrite burial on oxygen (run 8) increases Early Paleozoic $\delta^{13}C$ and removing the sulfur cycle altogether (run 9) increases it further. Both predictions agree less with the record than the baseline.

Changing the functional representation of carbon isotope fractionation (fig. 8D) affects the $\delta^{13}C$ predictions without altering any of the other model predictions. One possible explanation of the low $\delta^{13}C$ relative to the record in the Permian and Early Mesozoic, as well as in the last 30 million years, is that these are the periods of 'aragonite seas', characterized by high Mg:Ca ratio, in which aragonite and especially high-Mg calcite were buried in abundance (Sandberg, 1983; Hardie, 1996; Stanley and Hardie, 1998). While the burial of carbonate as aragonite would have caused a small increase in $\delta^{13}C$ in itself, the high-Mg calcite burial and $MgSO_4$ deposition would have other effects on carbonate burial which were not studied here (Morse and others, 1997; Stanley and Hardie, 1998). Run 10 assumes that in periods of 'aragonite seas' (335—180 MaBP and 30 MaBP—present), all $CaCO_3$ was buried as aragonite rather than calcite, with its stronger ^{13}C fractionation. This procedure improves the model predictions, but $\delta^{13}C$ is still low in the Permian and at present.

In run 11, the pO_2 effect on carbon isotope fractionation (Berner and others, 2000) is removed. This removal raises early Phanerozoic $\delta^{13}C$ and lowers later $\delta^{13}C$, removing the sustained Carboniferous maximum, resulting in a significantly worse prediction.

Phanerozoic $\delta^{34}S$

Figure 9 shows COPSE predictions of Phanerozoic $\delta^{34}S$, compared to the record of Strauss (1999). As with $\delta^{13}C$, the overall trend is successfully recreated, although the finer detail is not. In the baseline run 1, the main features are a significant drop of ~20 permil with the advent of land plants, and a slow uneven rise in the Mesozoic and Cenozoic. Unlike $\delta^{13}C$, the overall amplitude of $\delta^{34}S$ change is well captured, although Early Paleozoic predictions are a few permil too high. The timing of the predicted minimum of $\delta^{34}S$ in the Early Permian is rather early. Furthermore, the sharp Devonian minimum and Devonian/Carboniferous maximum that appear in the record of Claypool and others (1980) are missing. As with the absent Devonian $\delta^{13}C$ peak, these discreprancies could be due to inaccurate modeling of early vascular land plants.

The inclusion of the VCI feedback (run 2) seems to improve the Early Paleozoic $\delta^{34}S$ predictions. However, the total amplitude of change is reduced, and this prediction is not clearly better or worse than the baseline. Removing the dependency of S and C oxidative weathering on pO_2 (run 3) gives unrealistically large $\delta^{34}S$ variation, with early Paleozoic predictions being especially high. Removing the oxygen dependency of pyrite burial (run 8) reduces the amplitude of $\delta^{34}S$ change to less than that of the record.

Including a pO_2 dependency of ^{34}S fractionation in pyrite burial (run 12) gives the smallest amplitude of $\delta^{34}S$ variation of ~9 permil, with low Early Paleozoic values. This pO_2 dependent fractionation was taken from Berner and others (2000), as was the photosynthetic ^{13}C fractionation dependency on pO_2, which improved $\delta^{13}C$ predictions. However, the ^{13}C fractionation dependency is based on laboratory experiments on vascular land plants and marine phytoplankton, whereas the bacterial reducing-reducing ^{34}S fractionation is assumed to vary linearly with pO_2, with no experimental backing. The assumed function doubles fractionation from a reasonable 35 permil at present to a questionably high 70 permil at pO_2 = 2PAL, which is the approximate pO_2 maximum predicted by Berner and others (2000) in the Carboniferous. Other models use a constant 35 permil fractionation (for example, Kump and Garrels, 1986; Petsch and Berner, 1998).

The model's predicted isotope trends correctly reproduce the long-term inverse relationship between $\delta^{13}C$ and $\delta^{34}S$. This behavior is attributed to the coupled oxidation-reduction systems of the carbon and sulfur cycles, with times of abundant reduced sulfur deposition correlating with increased deposition of carbonate carbon (Holser and others, 1988).

DISCUSSION

The COPSE model can produce reasonable simultaneous predictions of coupled biogeochemical variables including pO_2, pCO_2, $\delta^{13}C$ and $\delta^{34}S$. Some previous models have used $\delta^{13}C$ and $\delta^{34}S$ isotope records as forcing functions, but the use of these records involves a number of auxiliary assumptions. The prediction of the two Phanerozoic isotope records is a novel feature, although there have been model predictions of carbon and strontium isotopes for the Cretaceous and Cenozoic (Wallmann, 2001; Hansen and Wallmann, 2003). Comparing COPSE model predictions with multiple independent datasets helps us to evaluate whether particular functional connections and/or feedbacks may have played an important role in determining Phanerozoic Earth system behavior.

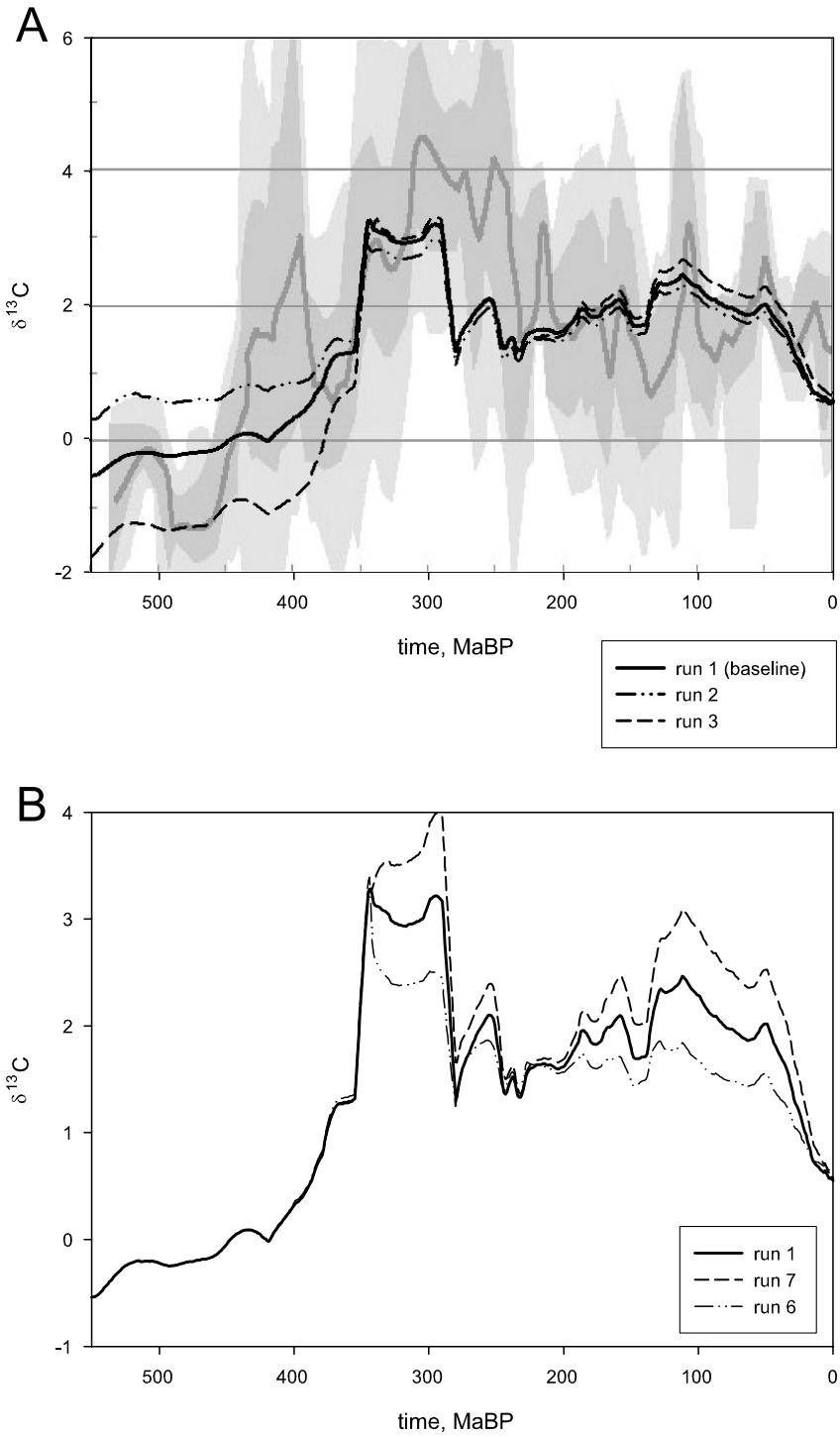

Fig. 8. COPSE model $\delta^{13}C$ predictions. (A) Changing O_2 feedbacks (runs 1, 2 and 3) effect on $\delta^{13}C$ prediction, compared with the record of Veizer and others (1999) – faded thick line, with darker and lighter shaded areas showing the 68% ($\pm\sigma$) and the 95% ($\pm 2\sigma$) probability, respectively. (B) Fire feedback effect on $\delta^{13}C$ (runs 1, 6 and 7). (C) Sulfur cycle variation effect on $\delta^{13}C$ (runs 1, 8 and 9). (D) Carbon isotope fractionation variations (runs 1, 10 and 11).

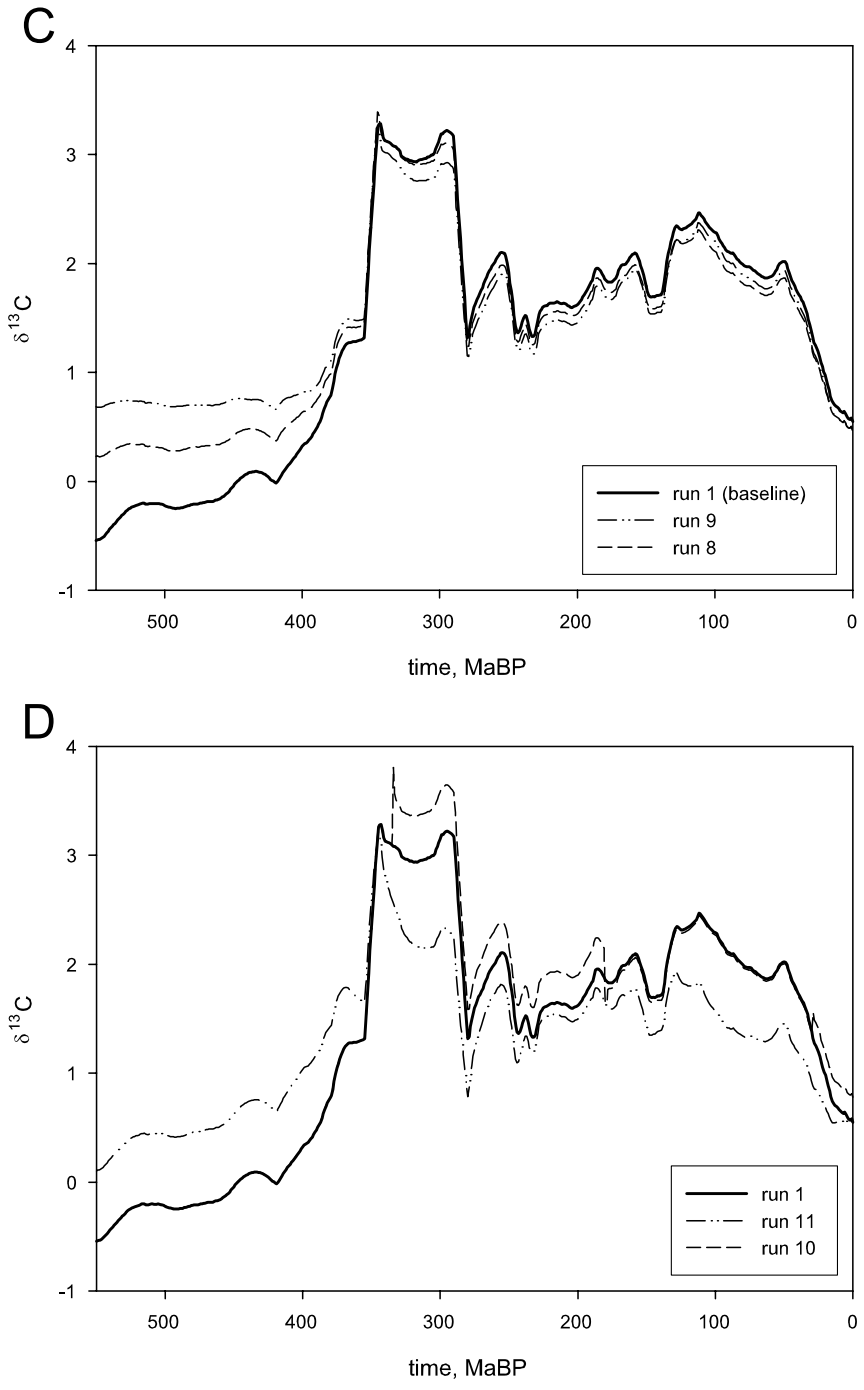

Fig. 8. (continued)

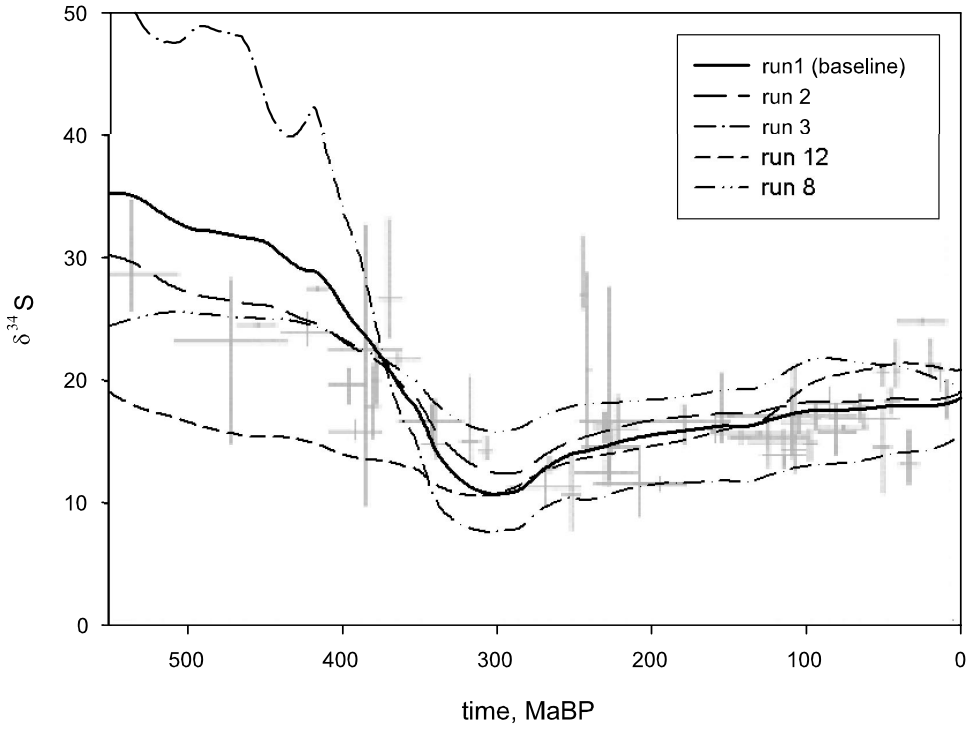

Fig. 9. COPSE model $\delta^{34}S$ predictions compared with the record of Strauss (1999). The record is marked by faded crosses, with vertical bars indicating $\delta^{34}S$ range and horizontal bars age uncertainty. COPSE runs shown are: runs 1 (baseline), 2 (VCI feedback), 3 (no oxidative weathering feedback), 8 (no pyrite burial feedback) and 12 ($\delta^{34}S$ fractionation dependent on O_2).

The COPSE model pO_2 predictions contrast with earlier models (Berner and Canfield, 1989; Berner and others, 2000). In the Paleozoic, pO_2 predictions are lower. After the establishment of land plants, most runs show a higher pO_2 peak in the Cretaceous than the Permo-Carboniferous, despite a doubling of the C:P burial ratio of terrestrial organic matter in the Permo-Carboniferous. The Cretaceous pO_2 peak is caused primarily by tectonic forcing, in particular, high metamorphic and volcanic degassing rates driving increased CO_2, phosphorus weathering and productivity. This feature is less marked in other oxygen models probably because they do not include tectonic forcing or the coupling between the carbon, phosphorus and oxygen cycles.

However, the height of the Cretaceous pO_2 peak, as well as the lack of an oceanic sulfate minimum and calcium maximum in this period, might be a model artifact due to the oversimplification of the sulfur cycle. Including volcanic sulfur inputs (degassing) and hydrothermal circulation (basalt-seawater exchange) in the model may resolve this problem: the mid-Cretaceous period had enhanced volcanic activity, which would have increased oxygen consumption (Hansen and Wallmann, 2003).

Our study suggests that a number of feedbacks may have operated together to regulate pO_2 over Phanerozoic time. The strong VCI pO_2 feedback of the marine C:P burial ratio raises early Phanerozoic pO_2, giving predictions closer to existing models (Berner and Canfield, 1989; Berner and others, 2000; Lenton, 2001). However, the $\delta^{13}C$ predictions are noticeably worse, and an unlikely organic C burial trend is generated. After the advent of land plants the VCI feedback has little impact because the ocean is generally lacking in anoxia (with the exception of known Oceanic Anoxic

Events). Our results suggest that the VCI feedback is weaker than originally proposed, in accord with recent measurements (Anderson and others, 2001). Oxygen regulation is possible without the VCI feedback through a combination of other mechanisms. One important feature is C-S-O coupling, including an inverse dependency of pyrite burial on pO_2, which allows oxygen to be 'shuttled' back and forth between the large reservoirs of carbonate carbon and gypsum sulfur. Fire feedbacks on phosphorus weathering and the apportioning of phosphorus between the land and the ocean prove important in regulating pO_2 after the advent of land plants. Removing any fire effect on terrestrial vegetation leads to poor pO_2 regulation, and only a minor improvement in pCO_2 and $\delta^{13}C$ predictions. We see no convincing theoretical reason for *completely* removing it. Strengthening the fire feedback brings pO_2 predictions within stringent constraints suggested previously (LW2; Lenton, 2001) but degrades the $\delta^{13}C$ prediction. Thus we opt for an intermediate strength of fire feedback and a pO_2 upper limit of 1.6 PAL (corresponding to 30vol%).

The COPSE model pCO_2 predictions are similar to the predictions of the Geocarb models (B1, B2, Berner and Kothavala, 2001) and, more importantly, they are broadly consistent with proxies, although there is disagreement amongst these in some intervals. In the Permo-Carboniferous, pCO_2 does not fall as low as in other models and some proxies. However, the model yields semi-quantitative temperature predictions that are lower than present, in line with evidence for glaciations. It is more difficult to generate low pCO_2 in the Permo-Carboniferous in our model than in Berner's work because of C-O coupling. Photosynthetic carbon fixation and hence plant productivity are directly related to pCO_2 and inversely related to pO_2. In the Carboniferous, both increasing pO_2 and decreasing pCO_2 tend to suppress productivity and weathering. The suppression of productivity generates two negative feedbacks: a reduction in the CO_2 sink from silicate weathering, and a reduction in the O_2 source from phosphorus weathering. The higher-than-present pO_2 and lower-than-present solar luminosity should both lead to a higher set point for pCO_2.

In some additional model runs oceanic CO_2 species and (carbonate) alkalinity were tracked, allowing calculation of atmospheric CO_2 from total atmosphere + ocean CO_2, temperature and alkalinity (rather than assuming a constant airborne fraction of atmosphere + ocean CO_2). Atmospheric pCO_2 predictions were *virtually unchanged*, while total atmosphere + ocean CO_2 variations were significantly dampened. This result implies that the small atmospheric pCO_2 repository acts more as a parameter indicating the state of the system than as an independent reservoir. Although the CO_2 reservoir division is more realistic, this method was not included in the COPSE baseline because the model's ocean chemistry was thought inadequate to yield meaningful predictions for the oceanic carbonate system.

The COPSE model was not expected to perfectly reproduce the geological records of $\delta^{13}C$ and $\delta^{34}S$, but major trends can be reproduced. Berner and others (2000) pO_2 dependency of carbon fractionation improves the $\delta^{13}C$ prediction, but their pO_2 dependency of sulfur fractionation severely degrades the $\delta^{34}S$ prediction. The pO_2 dependency of photosynthetic carbon fractionation is based on experimental evidence and biochemical understanding. The posited pO_2 dependency of sulfur fractionation in pyrite formation has no experimental basis and our study lends no support to it.

In general we found that C-O-S coupling is necessary to build a consistent model of Phanerozoic Earth system changes. Without the sulfur cycle, early pO_2 is too low, Carboniferous pCO_2 is too high, and $\delta^{13}C$ predictions are degraded.

The simple ocean biogeochemical cycling incorporated in COPSE shows promising results, with phosphate, nitrate, sulfate and calcium histories broadly in line with available evidence. The correlation between high $\delta^{13}C$ amplitude and periods of

aragonite and high Mg calcite deposition implies that the inclusion of full calcium and magnesium cycles would improve $\delta^{13}C$ predictions.

We stress that COPSE is work in progress. Future improvements and extensions to the model could include: a more detailed sulfur cycle, including volcanism (degassing), basalt-seawater interactions, and a differentiation between sulfur and carbon weathering processes; a more complete ocean chemistry, including carbonate chemistry, alkalinity and pH, calcium and magnesium; and paleogeographical data quantifying the effects of continental area and alignment on climate (temperature and runoff) and biological productivity.

CONCLUSIONS

From a modeling perspective, it is clear that coupled biogeochemical models, such as the one presented, have an important role in research of the Earth system: inclusion of known cycle couplings alters the behavior compared to 'single element' studies. However, better understanding of biogeochemical cycles and improved predictions require further geological, geochemical and paleontological evidence. We suggest addressing the following:

- Oxygen is most likely regulated by a combination of several feedbacks. Improved pO_2 predictions therefore require better assessment or more conclusive evidence of possible feedbacks, some of which are hotly contested:
  - How does oxidative weathering vary with pO_2, if at all?
  - How does marine organic C:P burial ratio vary with bottom water anoxia?
  - How does pyrite burial vary with pO_2 / anoxia?
  - How strong is the fire feedback on terrestrial productivity?
- Proxies for Phanerozoic pO_2, or at least better constraints, are needed. The Early Paleozoic (pre-vascular land plants) is especially poorly constrained, showing a large variation between different model predictions. From 350 MaBP to present, the continuous charcoal record offers evidence, but its interpretation as a pO_2 constraint still varies.
- CO_2 seems to be more 'hardwired' than O_2, being more dependent on the external forcings, and less on the dynamics of the model. Improved predictions of pCO_2 history therefore require better assessment of geological and tectonic forcings such as degassing and uplift rates. Also, the silicate weathering dependency on pCO_2 (f_{CO_2}) can affect the C cycle and therefore pCO_2 history and needs to be better constrained for different periods.
- Improved paleontological knowledge of isotope fractionation by terrestrial and marine biota could improve $\delta^{13}C$ predictions. A better understanding of ocean chemistry over the Phanerozoic, specifically the oceanic Ca and Mg cycles, and their effect on minerals deposited and their respective fractionation is also needed.

ACKNOWLEDGMENTS

We thank Rolf Arvidson, Robert Berner, Klaus Wallmann and an anonymous reviewer for their constructive reviews. We also thank Rob Raiswell and Julian Andrews for their helpful comments. The COPSE model code (programmed in C++) is available from Noam Bergman.

APPENDIX 1

Model Constants and Fluxes

TABLE 4

COPSE *model constants. KG86 = Kump and Garrels (1986); B1 = Berner (1991); LW1, LW2 = Lenton and Watson (2000a, 2000b).*

Const.	**Meaning**	**Baseline size**	**Source**
k_1	initial oxic fraction	0.86	LW1
k_2	Marine organic carbon burial	$4.50 \cdot 10^{12}$ mol C yr^{-1}	Bergman (ms, 2003)
k_3	nitrogen fixation	$8.72 \cdot 10^{12}$ mol N yr^{-1}	for steady state
k_4	denitrification	$4.3 \cdot 10^{12}$ mol N yr^{-1}	LW1
k_5	land organic carbon burial	$4.50 \cdot 10^{12}$ mol C yr^{-1}	Bergman (ms, 2003)
k_6	Fe-sorbed P burial	$0.6 \cdot 10^{10}$ mol P yr^{-1}	LW1
k_7	Ca-bound P burial	$1.5 \cdot 10^{10}$ mol P yr^{-1}	LW1
k_{10}	(reactive) P weathering	$4.35 \cdot 10^{10}$ mol P yr^{-1}	for steady state
k_{11}	fraction of P buried on land	0.10345	for steady state
k_{12}	carbonate carbon degassing	$6.65 \cdot 10^{12}$ mol C yr^{-1}	B1
k_{13}	organic carbon degassing	$1.25 \cdot 10^{12}$ mol C yr^{-1}	B1
k_{14}	carbonate weathering	$13.35 \cdot 10^{12}$ mol C yr^{-1}	B1
k_{15}	normalized pre-plant weathering	0.15	B1
k_{16}	conversion factor from normalized O_2 reservoir **o** to atmospheric pressure: $pO_2(atm) = \frac{\mathbf{o}}{\mathbf{o} + k_{16}}$	3.762	LW2
k_{17}	oxidative weathering of carbon	$7.75 \cdot 10^{12}$ mol C yr^{-1}	for steady state
k_{21}	pyrite (reduced) sulfur weathering	$0.53 \cdot 10^{12}$ mol S yr^{-1}	KG86
k_{22}	gypsum (oxidized) sulfur weathering	$1.0 \cdot 10^{12}$ mol S yr^{-1}	KG86
k_{fire}	fire frequency parameter	100	Bergman (ms, 2003)

TABLE 5

COPSE *fluxes taken directly from the Redfield Revisted (LW1, LW2) ocean model*

Flux	Modeled process	Present size/value	Baseline equation
newp	marine new production	225.96 mol kg^{-1} yr^{-1}	$117 \cdot \min(\mathbf{N}/16, \mathbf{P})$
anox	ocean anoxic fraction	0.14	$1 - k_1 \cdot \mathbf{o} \cdot newp'$
nfix	nitrogen fixation	$8.72 \cdot 10^{12}$ mol N yr^{-1}	$k_3 \left(\frac{\mathbf{P} - \mathbf{N}/16}{\mathbf{P}_0 - \mathbf{N}_0/16} \right)^2$
denit	denitrification	$8.6 \cdot 10^{12}$ mol N yr^{-1}	$k_4 \left(1 + \frac{anox}{1 - k_1} \right)$
fepb	iron-sorbed P burial	$6.0 \cdot 10^{9}$ mol P yr^{-1}	$k_6 \frac{1 - anox}{k_1}$
capb	calcium-bound P burial	$1.5 \cdot 10^{10}$ mol P yr^{-1}	$k_7 (newp')^2$

APPENDIX 2

The 'Friend' Feedback for Terrestrial Vegetation

This feedback is based on the inhibiting effect of oxygen on C_3 plants' photosynthesis, as O_2 competes with CO_2 for Rubisco sites. It follows the leaf photosynthesis models of Farquhar and others (1980) and Friend and others (1998), with the calculations of Friend (1998) adapted for the COPSE model (Bergman, ms, 2003). The Friend feedback requires an auxiliary calculation, with three model parameters: pO_2, pCO_2 and T. The basic calculation is:

$$V'_{npp} = \frac{V_{c,max}(\mathbf{a}'' - \Gamma)}{\mathbf{a}'' + K_c(1 + \mathbf{o}''/K_o)} \tag{52}$$

$$V_{npp} = k_{normal} \cdot V'_{npp} \cdot \boldsymbol{E}. \tag{53}$$

$V_{c,max}$ and $V_{o,max}$ represent the maximum velocities of carboxylation and oxygenation, respectively. $\mathbf{a}''$ and $\mathbf{o}''$ are $\mathbf{a}$ (atmospheric pCO_2) and $\mathbf{o}$ (atmospheric pO_2) in ppm, although in Friend's calculation they represent CO_2 and O_2 concentrations in the chloroplast, respectively. K_c and K_o are the Michaelis-Menten constants for the reaction in which CO_2 and O_2 are substrates competing for the enzyme Rubisco. k_{normal} normalizes V_{npp} to 1 for present level O_2, CO_2 and temperature. Γ is the CO_2 compensation mixing ratio for photosynthesis in the absence of day respiration. It is calculated as:

$$\Gamma = \frac{K_c}{2K_o} \cdot \frac{V_{o,\max}}{V_{c,\max}} \cdot \mathbf{o}'' \tag{54}$$

The 'constants' $V_{c,max}$, $V_{o,max}$, K_c and K_o all increase exponentially with temperature. They were calculated using Arrhenius Law, ignoring changes in atmospheric pressure. The calculation for each parameter is:

$$parameter = e^{(c - E_a/RT)} \tag{55}$$

where c is the appropriate rate constant and E_a the activation energy, using the values in table 6. R is the universal gas constant, and T is measured in Kelvin. In runs using a 'temperature-independent' Friend feedback T_0 (15°C) was used in all the calculations of equation 55.

TABLE 6

Constants for Arrhenius Law calculations of Michaelis-Menten constants and maximum carboxylation and oxygenation velocities, used in auxiliary calculation of land net primary productivity. Numbers from Friend (1998).

Parameter	Rate Constant (c)	Activation Energy (Ea), $J \cdot mol^{-1}$
K_c	39.63	84,200.0
K_o	19.11	15,200.0
$V_{c,max}$	33.30	82,000.0
$V_{o,max}$	17.60	44,000.0

REFERENCES

Anderson, L. D., Delaney, M. L., and Faul, K. L., 2001, Carbon to phosphorus ratios in sediments: Implications for nutrient cycling: Global Biogeochemical Cycles, v. 15, p. 65–79.

Beerling, D. J., Woodward, F. I., Lomas, M. R., Wills, M. A., Quick, W. P., and Valdes, P. J., 1998, The influence of Carboniferous palaeoatmospheres on plant function: an experimental and modelling assessment: Philosophical Transactions of the Royal Society of London, Biological Sciences, v. 353, p. 131–140.

Beerling, D. J., Lake, J. A., Berner, R. A., Hickey, L. J., Taylor, D. W., and Royer, D. L., 2002, Carbon isotope evidence implying high O_2/CO_2 ratios in the Permo-Carboniferous atmosphere: Geochimica et Cosmochimica Acta, v. 66, p. 3757–3767.

Bergman, N. M., ms, 2003, COPSE: A New Biogeochemical Model for the Phanerozoic: School of Environmental Sciences, Norwich, University of East Anglia, p. 197.

Berner, R. A., 1991, A model for atmospheric CO_2 over Phanerozoic time: American Journal of Science, v. 291, p. 339–376.

——— 1994, Geocarb II: A revised model of atmospheric CO_2 over Phanerozoic time: American Journal of Science, v. 294, p. 56–91.

——— 1998, The carbon cycle and CO_2 over Phanerozoic time: the role of land plants: Philosophical Transactions of the Royal Society of London: Biological Sciences, v. 353, p. 75–82.

Berner, R. A., and Canfield, D. E., 1989, A new model for atmospheric oxygen over Phanerozoic time: American Journal of Science, v. 289, p. 333–361.

Berner, R. A., and Kothavala, Z., 2001, Geocarb III: A revised model of atmospheric CO_2 over Phanerozoic time: American Journal of Science, v. 301, p. 182–204.

Berner, R. A., Lasaga, A. C., and Garrels, R. M., 1983, The carbonate-silicate geochemical cycle and its effect on atmospheric carbon dioxide over the past 100 million years: American Journal of Science, v. 283, p. 641–683.

Berner, R. A., Petsch, S. T., Lake, J. A., Beerling, D. J., Popp, B. N., Lane, R. S., Laws, E. A., Westley, M. B., Cassar, N., Woodward, F. I., and Quick, W. P., 2000, Isotope Fractionation and Atmospheric Oxygen: Implications for Phanerozoic O_2 Evolution: Science, v. 287, p. 1630–1633.

Brennan, S. T., and Lowenstein, T. K., 2002, The major-ion composition of Silurian seawater: Geochimica et Cosmochimica Acta, v. 66, p. 2683–2700.

Burke, W. H., Denison, R. E., Hetherington, E. A., Koepnick, R. B., Nelson, H. F., and Otto, J. B., 1982, Variation of seawater $^{87}Sr/^{86}Sr$ throughout Phanerozoic time: Geology, v. 10, p. 516–519.

Caldeira, K., and Kasting, J. F., 1992, The life span of the biosphere revisited: Nature, v. 360, p. 721–723.

Cerling, T. E., 1991, Carbon dioxide in the atmosphere: evidence from Cenozoic and Mesozoic paleosols: American Journal of Science, v. 291, p. 377–400.

Claypool, G. E., Holser, W. T., Kaplan, I. R., Sakai, H., and Zak, I., 1980, The age curves of sulfur and oxygen isotopes in marine sulfate and their mutual interpretation: Chemical Geology, v. 28, p. 199–260.

Colman, A. S., Mackenzie, F. T., and Holland, H. D., 1997, Redox Stabilisation of the Atmosphere and Oceans and Marine Productivity: Science, v. 275, p. 406–407.

Cressler, W. L., 2001, Evidence of earliest known wildfires: Palaios, v. 16, p. 171–174.

Derry, L. A., and France-Lanord, C., 1996, Neogene growth of the sedimentary organic carbon reservoir: Paleoceanography, v. 11, p. 267–275.

Dudley, R., 2000, The evolutionary physiology of animal flight: paleobiological and present perspectives: Annual Review of Physiology, v. 62, p. 135–155.

Ekart, D. D., Cerling, T. E., Montañez, I. P., and Tabor, N. J., 1999, A 400 million year carbon isotope record of pedogenic carbonates: implications for paleoatmospheric carbon dioxide: American Journal of Science, v. 299, p. 805–827.

Engebretson, D. C., Kelley, K. P., Cashman, H. J., and Richards, M. A., 1992, 180 million years of subduction: GSA Today, v. 2, p. 93–100.

Farquhar, G. D., von Caemmerer, S., and Berry, J. A., 1980, A biochemical model of photosynthetic CO_2 assimilation in leaves of C_3 species: Planta, 149, p. 78–90.

Farquhar, G. D., O'Leary, M. H., and Berry, J. A., 1982, On the relationship between carbon isotope discrimination and the intercellular carbon dioxide concentration in leaves: Australian Journal of Plant Physiology, v. 9, p. 121–137.

Frakes, L. A., 1979, Climates Throughout Geologic Time: Amsterdam, Elsevier Scientific Publishing Co., 310 p.

Freeman, K. H., and Hayes, J. M., 1992, Fractionation of carbon isotopes by phytoplankton and estimates of ancient CO_2 levels: Global Biogeochemical Cycles, v. 6, p. 185–198.

Fridovich, I., 1977, Oxygen is Toxic!: BioScience, v. 27, p. 462–466.

——— 1998, Oxygen toxicity: a radical explanation: Journal of Experimental Biology, v. 201, p. 1203–1209.

Friend, A. D., 1998, Appendix: Biochemical modelling of leaf photosynthesis, *in* Jarvis, P. G., editor, European forests and global change: Cambridge, Cambridge University Press, p. 335–346.

Friend, A. D., Kellomäki, S., and Kruijt, B., 1998, Modelling leaf, tree and forest responses to increasing atmospheric CO_2 and temperature, *in* Jarvis, P. G., editor, European forests and global change: Cambridge, Cambridge University Press, p. 293–334.

Gaffin, S., 1987, Ridge volume dependence on seafloor generation rate and inversion using long term sealevel change: American Journal of Science, v. 287, p. 596–611.

Garrels, R. M., and Lerman, A., 1981, Phanerozoic cycles of sedimentary carbon and sulfur: Proceedings of the National Academy of Sciences USA, v. 78, p. 4652–4656.

——— 1984, Coupling of the sedimentary sulfur and carbon cycles - an improved model: American Journal of Science, v. 284, p. 989–1007.

Garrels, R. M., and Perry, E. A., Jr., 1974, Cycling of carbon, sulfur, and oxygen through geologic time, The Sea: New York, Wiley, p. 303–336.

Guidry, M. W., and Mackenzie, F. T., 2000, Apatite weathering and the Phanerozoic phosphorus cycle: Geology, v. 28, p. 631–634.

Hansen, K. W., and Wallmann, K., 2003, Cretaceous and Cenozoic evolution of seawater composition, atmospheric O_2 and CO_2: A model perspective: American Journal of Science, v. 303, p. 94–148.

Hardie, L. A., 1996, Secular variation in seawater chemistry: an explanation for the coupled secular variations in the mineralogies of marine limestone and potash evaporites over the past 600 m.y.: Geology, v. 24, p. 279–283.

Hayes, J. M., Popp, B. N., Takigiku, R., and Johnson, M. W., 1989, An isotopic study of biogeochemical relationships between carbonates and organic carbon in the Greenhorn Formation: Geochimica et Cosmochimica Acta, v. 53, p. 2961–2972.

Hayes, J. M., Strauss, H., and Kaufman, A. J., 1999, The abundance of 13C in marine organic matter and isotopic fractionation in the global biogeochemical cycle of carbon during the past 800 Ma: Chemical Geology, v. 161, p. 103–125.

Holland, H. D., 1978, The Chemistry of the Atmosphere and Oceans: New York, John Wiley and Sons, 351 p.

——— 1984, The Chemical Evolution of the Atmosphere and Oceans: Princeton Series in Geochemistry: Princeton, Princeton University Press, 598 p.

——— 2003, Discussion of the article by A. C. Lasaga and H. Ohmoto on "The oxygen geochemical cycle: Dynamics and stability": Geochimica et Cosmochimica Acta, v. 67, p. 787–789.

Holser, W. T., Schidlowski, M., Mackenzie, F. T., and Maynard, J. B., 1988, Geochemical cycles of carbon and sulfur, *in* Gregor, C. B., Garrels, R. M., Mackenzie, F. T., and Maynard, J. B., editors, Chemical cycles in the Evolution of the Earth: New York, Wiley-Interscience, p. 105–173.

Horita, J., Zimmermann, H., and Holland, H. D., 2002, Chemical evolution of seawater during the Phanerozoic: Implications for the record of marine evaporites: Geochimica et Cosmochemica Acta, v. 66, p. 3733–3756.

Kump, L. R., 1988, Terrestrial feedback in atmospheric oxygen regulation by fire and phosphorus: Nature, v. 335, p. 152–154.

——— 1993, The coupling of the carbon and sulfur biogeochemical cycles over Phanerozoic time, *in* Wollast, R., Mackenzie, F. T., and Chou, L., editors, Interactions of C, N, P and S Biogeochemical Cycles and Global Change: NATO ASI: Berlin, Springer-Verlag, p. 475–490.

Kump, L. R., and Garrels, R. M., 1986, Modelling atmospheric O_2 in the global sedimentary redox cycle: American Journal of Science, v. 286, p. 337–360.

Kump, L. R., and Mackenzie, F. T., 1996, Regulation of Atmospheric O_2: Feedback in the Microbial Feedbag: Science, v. 271, p. 459–460.

Lasaga, A. C., and Ohmoto, H., 2002, The oxygen geochemical cycle: Dynamics and stability: Geochimica et Cosmochimica Acta, v. 66, p. 361–381.

Lenton, T. M., 2001, The role of land plants, phosphorus weathering and fire in the rise and regulation of atmospheric oxygen: Global Change Biology, v. 7, p. 613–629.

Lenton, T. M., and Watson, A. J., 2000a, Redfield revisited: 1. Regulation of nitrate, phosphate and oxygen in the ocean: Global Biogeochemical Cycles, v. 14, p. 225–248.

——— 2000b, Redfield revisited: 2. What regulates the oxygen content of the atmosphere?: Global Biogeochemical Cycles, v. 14, p. 249–268.

McArthur, J. M., Howarth, R. J., and Bailey, T. R., 2001, Strontium isotope stratigraphy: LOWESS version 3: best fit to the marine Sr-isotope curve for 0-509 Ma and accompanying look-up table for deriving numerical age: Journal of Geology, v. 109, p. 155–170.
McElwain, J. C., and Chaloner, W. G., 1995, Stomatal density and index of fossil plants track atmospheric carbon dioxide in the Palaeozoic: Annals of Botany, v. 76, p. 389–395.
Mook, W. G., 1986, ^{13}C in atmospheric CO_2: Netherlands Journal of Sea Research, v. 20, p. 211–223.
Mora, C. I., Driese, S. G., and Colarusso, L. A., 1996, Middle to late Paleozoic atmospheric CO_2 levels from soil carbonate and organic matter: Science, v. 271, p. 1105–1107.
Morse, J. W., Wang, Q., and Tsio, M. Y., 1997, Influences of temperature and Mg:Ca ratio on $CaCO_3$ precipitates from seawater: Geology, v. 25, p. 85–87.
Pearson, P. N., and Palmer, M. R., 2000, Atmospheric carbon dioxide concentrations over the past 60 million years: Nature, v. 406, p. 695–699.
Petsch, S. T., and Berner, R. A., 1998, Coupling the geochemical cycles of C, P, Fe, and S: The effect on atmospheric O_2 and the isotopic records of carbon and sulfur: American Journal of Science, v. 298, p. 246–262.
Popp, B. N., Takigiku, R., Hayes, J. M., Louda, J. W., and Baker, E. W., 1989, The post-Paleozoic chronology and mechanism of $\delta^{13}C$ depletion in primary marine organic matter: American Journal of Science, v. 289, p. 436–454.
Raiswell, R., and Berner, R. A., 1986, Pyrite and organic matter in Phanerozoic normal marine shales: Geochimica et Cosmochimica Acta, v. 50, p. 1967–1976.
Raymo, M. E., 1997, Carbon Cycle Models: How Strong are the Constraints?, *in* Ruddiman, W. F., editor, Tectonic Uplift and Climate Change: New York, Plenum Press, p. 367–381.
Rees, C. E., 1970, The sulphur isotope balance of the ocean: an improved model: Earth and Planetary Science Letters, v. 7, p. 366–370.
Robinson, J. M., 1989, Phanerozoic O_2 variation, fire, and terrestrial ecology: Palaeogeography, Palaeoclimatology, Palaeoecology (Global and Planetary Change Section), v. 75, p. 223–240.
Ronov, A. B., 1976, Global carbon geochemistry, volcanism, carbonate accumulation, and life: Geochemistry International, v. 13, p. 172–195.
Sandberg, P. A., 1983, An oscillating trend in Phanerozoic non-skeletal carbonate mineralogy: Nature, v. 305, p. 19–22.
Stanley, S. M., 1999, Earth System History: New York, W. H. Freeman and Company, 615 p.
Stanley, S. M., and Hardie, L. A., 1998, Secular oscillations in the carbonate mineralogy of reef-building and sediment-producing organisms driven by tectonically forced shifts in seawater chemistry: Palaeogeography, Palaeoclimatology, Palaeoecology (Global and Planetary Change Section), v. 144, p. 3–19.
Strauss, H., 1999, Geological evolution from isotope proxy signals - sulfur: Chemical Geology, v. 161, p. 89–101.
Van Cappellen, P., and Ingall, E. D., 1994, Benthic phosphorus regeneration, net primary production, and ocean anoxia: A model of the coupled marine biogeochemical cycles of carbon and phosphorus: Paleoceanography, v. 9, p. 677–692.
——— 1996, Redox stabilisation of the Atmosphere and Oceans by Phosphorus-Limited Marine Productivity: Science, v. 271, p. 493–496.
Veizer, J., Holser, W. T., and Wilgus, C. K., 1980, Correlation of $^{13}C/^{12}C$ and $^{34}S/^{32}S$ secular variations: Geochimica et Cosmochimica Acta, v. 44, p. 579–587.
Veizer, J., Ala, D., Azmy, K., Bruckschen, P., Buhl, D., Bruhn, F., Carden, G. A. F., Diener, A., Ebneth, S., Godderis, Y., Jasper, T., Korte, C., Pawellek, F., Podlaha, O. G., and Strauss, H., 1999, $^{87}Sr/^{86}Sr$, $\delta^{13}C$ and $\delta^{18}O$ evolution of Phanerozoic seawater: Chemical Geology, v. 161, p. 59–88.
Volk, T., 1987, Feedbacks between weathering and atmospheric CO_2 over the last 100 million years: American Journal of Science, v. 287, p. 763–779.
——— 1989, Sensitivity of climate and atmospheric CO_2 to deep-ocean and shallow-ocean carbonate burial: Nature, v. 337, p. 637–640.
Walker, J. C. G., Hays, P. B., and Kasting, J. F., 1981, A negative feedback mechanism for the long-term stabilisation of Earth's surface temperature: Journal of Geophysical Research, v. 86, p. 9776–9782.
Wallmann, K., 2001, Controls on the Cretaceous and Cenozoic evolution of seawater composition, atmospheric CO_2 and climate: Geochimica et Cosmochimica Acta, v. 65, p. 3005–3025.
Watson, A. J., ms, 1978, Consequences for the Biosphere of Forest and Grassland Fires, Department of Cybernetics: Ph.D. thesis, Reading, United Kingdom, University of Reading, p. 276.
Yapp, C. J., and Poths, H., 1992, Ancient atmospheric CO_2 pressures inferred from natural goethites: Nature, v. 355, p. 342–344.